

Accepted Manuscript

Geochemistry: Exploration, Environment, Analysis

Supergene alteration, environmental impact and laboratory scale acid water treatment of Cyprus-type ore deposits: case study of Mathiatis and Sha abandoned mines

Evangelos Galanopoulos, Nikolaos Skarpelis & Ariadne Argyraki

DOI: <https://doi.org/10.1144/geochem2018-070>

Received 16 October 2018

Revised 23 January 2019

Accepted 29 January 2019

© 2019 The Author(s). Published by The Geological Society of London for GSL and AAG. All rights reserved. For permissions: <http://www.geolsoc.org.uk/permissions>. Publishing disclaimer: www.geolsoc.org.uk/pub_ethics

Supplementary material at <https://doi.org/10.6084/m9.figshare.c.4383254>

To cite this article, please follow the guidance at http://www.geolsoc.org.uk/onlinefirst#cit_journal

Manuscript version: Accepted Manuscript

This is a PDF of an unedited manuscript that has been accepted for publication. The manuscript will undergo copyediting, typesetting and correction before it is published in its final form. Please note that during the production process errors may be discovered which could affect the content, and all legal disclaimers that apply to the journal pertain.

Although reasonable efforts have been made to obtain all necessary permissions from third parties to include their copyrighted content within this article, their full citation and copyright line may not be present in this Accepted Manuscript version. Before using any content from this article, please refer to the Version of Record once published for full citation and copyright details, as permissions may be required.

Supergene alteration, environmental impact and laboratory scale acid water treatment of Cyprus-type ore deposits: Case study of Mathiatis and Sha abandoned mines

Supergene alteration-AMD treatment

Evangelos Galanopoulos*, Nikolaos Skarpelis & Ariadne Argyraki

Department of Economic Geology and Geochemistry, Faculty of Geology and Geoenvironment, National and Kapodistrian University of Athens, Panepistimiopolis Zographou, 15784, Athens, Greece

**Corresponding author (e-mail: egalanop@geol.uoa.gr)*

Abstract: Waste-rock dumps and the water quality of pit-lakes formed at abandoned mines of pyrite-rich ore deposits are of considerable environmental concern around the world. The Mathiatis and Sha mines provide typical examples of abandoned mines where Cyprus-type Cu-pyrite ore was exploited. Supergene alteration of the sulphide ore and the mine waste leads to the formation of efflorescence and generation of acid mine drainage filling the pit-lakes. Sulphate concentrations range from 4,600 to 4,850 mg/L and from 35,900 to 38,500 mg/L for the Mathiatis and Sha mines, respectively. Concentrations of heavy metals exceed the established regulatory limits in water. A preliminary assessment of the mine waste at the Mathiatis mine indicated that it cannot be characterized as inert material according to current European legislation, posing an environmental threat as a source of acid mine drainage (AMD). The identified Mg, Ca and Fe(II)- Fe(III) efflorescence mineral phases retain temporarily trace metals near the mine waste and the open pit-lake shore. Neutralisation experiments on the acidic waters of the epilimnion indicated local limestone is not sufficient for full remediation. However, it could be used as a low-cost pretreatment method for AMD. The study expands the international database of AMD affected areas and provides the basis for future remediation efforts.

Keywords: Mineral efflorescence; acid pit-lake; acid water treatment; Cyprus-type Cu-pyrite deposits

Supplementary material: Supplementary Table 1: Detection limits and Reference Material analyses is available at <https://doi.org/10.6084/m9.figshare.c.4383254>

Open-pit mining activities produce large volumes of mine waste exposed to weathering processes, usually generating an acidic environment with increased metal solubility (Changul *et al.* 2010; Chou I.-M. *et al.* 2013; Nieva *et al.* 2016; Nieva *et al.* 2018). The circulating solutions created can feed nearby open pit-lakes, or potentially affect aquifers, causing environmental concerns (Szczepanska & Twardowska 1999; Equeenuddin *et al.* 2010; Lei *et al.* 2010). These waters constitute Acid Mine Drainage (AMD) (Schmiermund & Drozd 1997; Seal & Shanks 2008; Romero *et al.* 2011; Favas *et al.* 2012; Soltani *et al.* 2014; Li *et al.* 2015; Favas *et al.* 2016). When mine waters are discharged into pit-lakes and streams, serious degradation of water quality may take place, with possible environmental effects on aquifers. The production of AMD is accredited primarily to the oxidation of sulphide minerals and most often to the oxidation of pyrite and pyrrhotite (Kelly 1991; Gray 1997; Chou *et al.* 2013) contained in the mine waste or in remnants of the mineralisation, whereas bacteria can contribute as catalysts accelerating the oxidation reactions (Nordstrom 2011). Once AMD is generated, it is challenging to control the process, as its treatment usually requires a high financial expenditure. Estimated cost of remediation for only the state of Pennsylvania in the USA using current technology, has been calculated to be up to 5 billion USD (US Geological Survey (USGS) 2010), while the estimated cost for the total worldwide liability associated with the current and future remediation of AMD is approximately 100 billion USD (Tremblay & Hogan 2001).

Treatment methods for AMD are divided into passive and active, based on the requirement for continuous or occasional input of chemical agent. Passive treatment options include aerobic or anaerobic wetlands (Machemer & Wildeman 1992), vertical flow wetlands, AMD treatment ponds, bioreactors and permeable reactive barriers (Kaur *et al.* 2018 and references therein). The most common method for AMD neutralisation is active treatment with the use of alkaline material increasing the pH and decreasing metal solubility. As a result, the metals in solution precipitate

either as hydroxides, sulphates or carbonates. Lime treatment is the most commonly used active treatment method, due to its efficiency and low cost (Potgieter-Vermaak *et al.* 2006). However, limestone is the most cost-effective neutralisation material available, but has not been used widely for AMD treatment, because of its slow rate of dissolution, tendency for armouring of grain surfaces (Hammarstrom *et al.* 2003) and production of voluminous sludge (Kaur *et al.* 2018).

AMD issues rise in areas with intense past mining activities such as the Iberian Pyrite Belt in south west Spain (Olias *et al.* 2004; Grande *et al.* 2014), the coal mines in India (Rawat & Singh 1982; Jamal *et al.* 1991) and Cyprus due to its well-known massive Cu-pyrite deposits. Large-scale copper production by exploitation and processing of copper ore gave Cyprus the ability to become the major producer and exporter of the metal in Eastern Mediterranean countries since the Late Bronze Age (Gale & Stos-Gale 1986; Kassianidou 2013). Silver was extracted as a byproduct of copper ore smelting. Production of copper is documented by impressive ancient metallurgical slag heaps, remains of ancient exploitation works and findings of ancient smelting furnaces, copper oxhide ingots (metal blocks resembling the shape of the hide of an ox) and ancient metallic objects (Hadjistavrinou & Constantinou 1982; Knapp *et al.* 2001; Kassianidou 2013). Ore exploitation was carried out mainly by open-pit mining. Flotation techniques were applied for the production of copper (mainly chalcopyrite) and pyrite concentrates, used for copper extraction and in the chemical industry respectively (Lavender 1962; Bear 1963). Production of copper- and pyrite-concentrates diachronically contributed significantly to the economy of the island and is directly linked with the welfare of the inhabitants. Today, copper and minor gold production takes place at Skouriotissa by Hellenic Copper Mines S.A. by application of acid leaching, solvent extraction and electrowinning techniques (USGS 2014).

As a result of the extensive mining activity and the closure of mines, abandoned open pits are scattered around Troodos Mt. (Fig. 1a), whereas mine waste spoils surround open pits. Open pits have been flooded with acidic water, while the mine waste spoils react with the environment releasing potentially toxic metals to the surrounding soils and the open-pit lakes. The increased

concentration of sulphates in the pit-lake water can also affect the local climate by producing low pH rainwater as observed by Charalambides *et al.* (2003), who found a strong correlation between increased sulphate concentrations and decreased pH in rainwater samples. Due to the absence of another sulphur emission source, the researchers proved the predominant effect of the Sha mine waste on the local atmospheric conditions. The acidic mine-pit lakes along with the mine waste spoils have been left untreated. Limited research has been conducted so far on the environmental impacts of exploitation of the Cyprus massive sulphide deposits (Charalambides *et al.* 1998; Hudson-Edwards & Edwards 2005; Ng & Malpas; 2013; Antivachis *et al.* 2017).

The present study contributes to the international database of AMD affected areas by presenting new data on the Mathiatis and Sha abandoned mines located at the NE foothills of Troodos Mt. (Fig. 1a). Both mines belong to the same mining district, located 23 Km south of Nicosia and 28 Km west of Larnaca, respectively. The two mines are typical examples of Cyprus-type Volcanogenic Massive Sulphide (VMS) mineralisation with good exposure and easy access to the remaining ore, host rock and mine waste. The objectives of the study are to investigate the mineralogy and geochemistry of weathering of hypogene ore and mine waste, as well as the chemistry of pit-lake water at the Mathiatis and Sha abandoned mines. The results of laboratory tests for neutralisation of AMD using limestone and lime as a neutralisation agent are also presented with the aim to investigate their performance for constraining the environmental impact of abandoned mines.

Geology of the study area

Cyprus-type Volcanogenic Massive Sulphides

The Cyprus mineralisation is classified as “Cyprus-type Volcanogenic Massive Sulphides” (VMS). Based on the work presented by Moussoulos (1957); Constantinou & Govett (1973); Adamides (1980); Constantinou (1980); Oudin & Constantinou (1984); Prichard & Maliotis (1998) and Herzig *et al.* (1991), the mineralisation is hosted within the extrusive volcanic sequence (Lower Pillow Lavas)

of the Late Cretaceous Troodos ophiolite, being genetically related to contemporaneous submarine hydrothermal activity. The ore bodies are fault controlled and mushroom-shaped, comprising a lens of massive sulphide ore consisting mainly of pyrite, chalcopyrite and minor bornite and sphalerite. Immediately beneath the massive pyritic lens, a complex network of quartz and sulphide veins - with pyrite as the predominant sulphide mineral - exists, cutting through intensively propylitised basalts. This complex network, with sulphur content between 15-35 wt%, narrows downwards and becomes poorer in pyrite. This association of pyrite and quartz veins is known as stockwork-type mineralisation which represents the feeder zone for the overlying massive sulphide lens. Most of the deposits are overlain by a manganese-poor, iron-rich sediment, which commonly contains sulphides (ochre) or/and manganese- and iron-rich sediment devoid of sulphides (umbers) and unmineralised Upper Pillow Lavas (Constantinou & Govett 1973; Robertson 1975; Adamides 1980; Constantinou 1980). The genesis of the deposits has been linked to hydrothermal activity at a spreading axis setting, similar to present-day equivalent settings on the ocean floor (e.g., the Trans-Atlantic Geotraverse (TAG) (Hannington *et al.* 1998) and the Mid-Atlantic Ridge (Rona 2005)). More than 30 massive sulphide ore bodies ranging in size between several thousands of tonnes to 16 million tonnes, with an average copper content between 0.5 to 4.5 wt%, have been mined in the Troodos ophiolite and many other exploration targets have been reported (Cyprus Geological Survey 2007; USGS, 2014).

Mathiatis

Mineral exploration at Mathiatis started in 1935 by Cyprus Mines Corporation (CMC) as part of a gold exploration program in Cyprus. Exploration works by Hellenic Mining Company (HMC) proved 2.8 Mt of pyrite ore with average sulphur and copper contents close to 28 and 0.23 wt% respectively. Open-pit mining up to 1987 resulted in production of 2 Mt of pyrite with concomitant production of 7 Mt of mine waste (Dr G. Maliotis 2010, pers. comm. to NS). The closure of the mine has left a deep pit now hosting an acid pit-lake fed by precipitation and surface runoff (Fig. 2a). As

presented by Charalambides *et al.* (1998) no effect of AMD has been traced in the nearby wells and irrigation boreholes.

The mineralisation at Mathiatis is controlled by two sub-parallel NW trending faults (Lydon & Galley 1986 and references therein) (Fig. 1b). The massive pyrite ore body had a lens-like form, overlaying a stockwork-type mineralisation consisting of quartz veining with disseminated pyrite mineralisation (Lydon 1984). Lydon & Galley (1986) claimed that the mineralisation was deposited on the slope of the paleotopography of the ocean. The massive pyrite body was stratigraphically overlain by amber and pillow lavas of the Upper sequence. The major part of the pyrite ore lens has been mined, leaving the stockwork mineralisation in the SE part of the open pit exposed to weathering.

Sha

Mineralisation at the Sha mine is controlled by NE faults crosscutting brecciated pillow lavas indicating they acted as channel conduits for hydrothermal fluids. Dykes of basalt crosscut the main fault zone (Fig. 1c). The ore body comprises a massive pyrite ore lens overlying a subeconomic stockwork-type pyrite mineralisation. The high-grade ore consisted of massive pyrite with a sulphur content higher than 40 wt% and minor chalcopyrite (average 0.5-1 Cu wt%) (Panayiotou 1968). Part of the massive sulphide ore body is left in situ. It was worked for gold and silver since 1943 and terminated in 1959. Massive ore lodes on the order of 170,000 tonnes with an average grade of 40 wt% sulphur and 0.5–1.0 wt% Cu and disseminated ore of about 164,000 tonnes with an average grade of 25 wt% sulphur and 0.2 wt% Cu were exploited (Dr G. Maliotis 2010, pers. comm. to NS). The waste material was estimated to be of the order of 6.5 million tonnes spread around an area of 14,000 m² (Charalambides *et al.* 1997). The flooded open pit with a max depth of 85m has an extent of roughly 4,400 m² (Fig. 2b).

Materials and Methods

Field sampling and sample preparation

Field sampling of ore, efflorescence material, mine waste and mine water took place in October 2011. Climatic conditions in the Mathiatis and Sha area are those of an intense semi-arid Mediterranean-type with a typical seasonal cycle. Precipitation in Cyprus during September and October 2011, as reported by the Cyprus Meteorological Service, was 20.2 and 14.5 mm, respectively. Maximum and minimum temperature during sampling for August, September and October ranged from 20.5–41.3 °C, 24.9–38.2 °C and 10.2–31.8 °C, respectively. The sampling locations are presented in Fig. 1b and 1c. Hand specimens of remaining ore were collected from the eastern slopes of Mathiatis and Sha open pits. Efflorescence was collected from the shore of the two pit-lakes with a plastic spatula. Samples of mine waste were taken from four different points of the mine spoils at the abandoned Mathiatis mine. An amount of material of roughly 5 kg was collected by channel techniques and sample mass was reduced by quartering to approximately 0.5 kg. In the laboratory, mine waste and ore samples were air dried and pulverized using a tungsten carbide automated mill in order to reach a grain size of <70µm prior to chemical analysis.

Pit-lake water samples were collected from the top 30 cm layer of the lakes (on the top of the epilimnion) by throwing 3L polyethylene containers from the coast into the water. After collection, a 50 ml aliquot of fluid was removed from each sample and filtered into a clean polyethylene bottle (using a 0.45 µm cellulose acetate disk filter attached to a disposable syringe to remove suspended particles) and acidified with concentrated nitric acid (supra pure grade) to avoid metal precipitation. An additional quantity of each non-acidified water sample was collected in 1L polyethylene bottles without leaving any headspace. All water samples were stored in a refrigerator at about 4–5°C to suspend biological and chemical reactions. In the laboratory, the 1L samples were filtered by using 0.45 µm pore cellulose filters and kept refrigerated for measuring the concentration of NO_3^- and SO_4^{2-} . Additionally, a sufficient quantity of untreated refrigerated pit-lake water was shipped to National

and Kapodistrian University of Athens (NKUA) immediately after collection in order to be used in the neutralisation experiments.

Neutralisation agents

The neutralisation agents used in the laboratory tests of the present study are commercial aggregates produced after processing of the Mitsero, Kaos and Latouros limestones (Fig. 1a). Quicklime (Ca(OH)_2) was also tested as a typical material used for neutralisation for comparison of the results. The Mitsero material is produced after processing of a Miocene coral limestone of the Koronia Formation (Follows 1992). It consists of calcite with subordinate dolomite. The Latouros material is quarried from the Nicosia formation, comprising chalk and marl (Palamakumbura & Robertson 2018). The minerals identified in the Latouros samples are mainly calcite and dolomite with minor K-feldspar, plagioclase, quartz and chromite. The Kaos agent is produced from the Aquitanian – Burdigalian Terra Member Formation, which is the upper part of the Pakhna Formation (Follows 1992). The material consists of dolomite and calcite, which in some occurrences can be Mg-calcite. The quicklime used in this study is produced after processing of limestone of the Koronia Formation.

Analytical Methods

Water samples

The physicochemical parameters of water samples, including temperature, electrical conductivity (EC), total dissolved solids (TDS) and pH/Eh were measured in situ with a multi-parameter EUTECH CyberScan PCD 650 instrument. The filtered and acidified water samples were commercially analysed by Inductively Coupled Plasma – Mass Spectrometry (ICP-MS) (ACME Labs, Canada) for trace elements. Analytical bias was assessed by analysing certified standard reference materials (TMDA-70 lake water) as shown in Supplementary Table 1 (S1). Nitrate concentrations were measured in non-acidified samples by ion chromatography in the Chemical Laboratory of the

Geological Survey Department of Cyprus and concentrations of SO_4^{2-} were measured on a HACH DR4000 spectrophotometer by application of the US-EPA (1978) 375.4 equivalent method at the Laboratory of Economic Geology and Geochemistry (LEGG), (NKUA).

Mine waste and ore samples

All were analysed at OMAC Labs, Ireland following aqua regia dissolution according to the ICP-ORE method for the ore samples and ME-MS41 method for the mine waste samples. Gold concentrations in the ore samples were determined using an acid attack on the samples followed by a methylisobutylketone extraction (Rubeska *et al.* 1977). Measurements were performed by using a Graphite Furnace Atomic Absorption Spectroscopy (GFAAS) Perkin–Elmer 1100B apparatus, at the LEGG-NKUA. Detection limits and reference material analyses are presented in Supplementary Table 1 (S1). Mineral identification of efflorescent salts was based on combined X-ray diffraction (XRD) and Scanning Electron Microscopy / Energy Dispersive X-Ray Spectroscopy (SEM/EDS) analyses. For XRD, a Siemens D-5005 diffractometer was used. All samples were scanned between 3 and 65° 2 θ angle with 1 °/min velocity, using the Ka radiation of a Cu x-ray tube, operated at a voltage of 40 kV and a current of 40 mA. X-ray diffractograms were evaluated with the EVA software, version 10.0. SEM-EDS analysis was carried out on carbon coated, resin impregnated or free surface samples, using a Jeol JSM 5600 SEM instrument, equipped with an Oxford ISIS 300 microanalytical device. Examination in the Backscattered Electron (BSE) mode permitted the localisation of metal enriched areas in the samples. The paste pH was measured according to USA-EPA (1996) method 9045C. The Net Neutralisation Potential (NNP) was calculated by subtracting the Acid Potential (AP) from the Neutralisation Potential (NP) according to the method US-EPA (1994), 2.2 Static Test method.

Neutralisation tests

The procedure followed in the neutralisation tests was based on the method proposed by Potgieter – Vermaak *et al.* (2006). According to their protocol, 5 g of each neutralisation agent were added to 50 ml of AMD in conical flasks. Two different grain sizes (<150 μm and <300 μm) of the limestone material were tested in order to identify any effect of specific surface area during

interaction. The solutions were placed on an orbital stirring table and left to react while stirring for 1 and 6 hours. After the predefined stirring time the samples were centrifuged for 10 minutes at 3,500 rpm and the supernatant was collected in clean test tubes after filtration with 0.45 µm membrane filters. The bottom sediment was collected and analysed following the same SEM-EDS technique as mentioned above. The solution was split into two, one for measurements and the other for safekeeping. After a first round of experimentation it was noted that the quantity of quicklime used had to be reduced in order to achieve the neutral pH target within one hour of reaction. The appropriate quantity was selected based on subsequent experimentation by varying the mixing ratio accordingly for the two pit-lake water samples.

Quantitative analysis of SO_4^{-2} in AMD before and after treatment was performed with a HACH DR4000 spectrophotometer at the LEGG-NKUA, using the equivalent of US-EPA (1978) 375.4 method for wastewater. The physicochemical parameters, i.e., pH and TDS, of solutions were monitored during treatment with the use of a Eutech PCD 650 polymeter apparatus calibrated with two pH buffers at 4 and 7. Trace metal concentrations after treatment were measured by Flame Atomic Absorption Spectroscopy (FAAS) using a Perkin – Elmer 1100B instrument.

Results

Ore mineralogy and geochemistry

The semi-massive to disseminated stockwork-type ore remaining on the eastern slope of the Mathiatis open pit consists of euhedral pyrite, marcasite and minor chalcopyrite. Pyrrhotite, sphalerite and barite are subordinate minerals, whereas quartz is the main gangue. The mean iron and sulphur contents of concentrates are 34.1 wt% and 39.0 wt%, respectively (Table 1), with copper content close to 0.1 wt%. Samples from the Sha sulphide ore body consist predominantly of massive, commonly porous and brecciated pyrite. Colloform pyrite with well-developed growth banding is a common textural feature. Individual colloform pyrite structures are cemented by chalcopyrite, marcasite and sphalerite. Black smoker structures have also been observed. Open tubes are

preserved indicating that part of the ore was formed within a black smoker field. The mean iron and sulphur concentrations of the Sha ore are 24.9 and 28.8 wt%, respectively (Table 1), with copper concentration close to 2.0 wt%. Average gold contents of analysed samples of Mathiatis and Sha ores are 0.4 mg/kg and 1.1 mg/kg, respectively. Although sampling was limited to small exposed parts of the ore bodies, a comparison with mean Au concentration from the TAG Mount (Hannington *et al.* 1991) indicates a low-grade mineralisation.

Characterization of the Mathiatis mine waste

The Mathiatis mine waste facility was developed to the east of the open-pit throughout the time of ore exploitation (Fig. 2c). The spoil is estimated to be of the order of 10.5 million tonnes (Charalambides *et al.* 1998) and consists of waste material ranging in size from fine clay particles to boulders exceeding 1m in diameter. The soil temperature measured at 16 different points varied from 24.2–27.0 °C.

Mine waste samples are classified as gravelly sand with some silt. The particles consist mainly of basalt, jasper and quartz with disseminated pyrite. Quartz, pyrite, plagioclase, chlorite, zeolite, gypsum, jarosite, natrojarosite, goethite, hematite and clay minerals of the smectite group are the major mineral components with minor goethite (Fig. 3).

Paste pH values from the mine waste samples vary from 2.2 to 4.7. Negative Net Neutralisation Potential values indicate the samples are acid generating (Table 2). Chemical analyses of mine waste samples showed high Fe, S, Zn, Pb, Co and As concentrations, reaching maximum concentrations of 20.4 wt%, 10.4 wt%, 1,351 mg/kg, 93.6 mg/kg, 74 mg/kg and 159.6 mg/kg, respectively. The observed values are related to the occurrence of sulphide ore minerals. A comparison against the Dutch intervention values (Swartjes 1999) exhibits an over the limit concentration of As and Cu. These As and Cu concentrations are also higher than the average topsoil values of Cyprus (Cohen *et al.* 2012) (Table 3).

A water drainage sample was collected from the surface run-off of mine waste stockpiles. The chemical analysis indicated pH values close to 2, high sulphate concentration exceeding 213,000

mg/L and concentrations of major and trace elements much higher in comparison with the samples from the open pits of Mathiatis and Sha (e.g., Fe around 37,000 mg/L, Mg 15,300 mg/L, Cu 480 mg/L and Zn 2,060 mg/L).

Efflorescence fields: Mode of occurrence and mineralogy

Mathiatis

Efflorescence on the shore of the Mathiatis pit-lake appears in a variety of colors from white to yellowish and orange (Fig. 2d). Gypsum is the most common supergene mineral in the studied area, while the other major minerals identified in the samples were hexahydrite and starkeyite. Copiapite, bloedite and pickeringite were detected at lesser proportions (Table 4; Fig. 4a).

An extensive efflorescence field is developed along the mine road to the top of the mine waste pile at Mathiatis (Fig. 2e). Thick crusts of sulphate salts appear in a plethora of colors. Close to the stagnant water level, the sulphates had a white to light blue color with tints of yellow, orange and light green. The major efflorescence minerals are gypsum, hexahydrite, copiapite, pickeringite and starkeyite, whereas tamarugite, halotrichite, metasideronatrite, pentahydrite, szomolnokite and alunogen are subordinate (Fig. 4b).

Sha

An extensive efflorescence field is developed at the expense of massive Cu-pyrite ore in the eastern part of the open pit, suggesting replacement of sulphides by sulphates. On the shores of the pit-lake a yellowish to brownish efflorescence crust has been formed on the ground surface (Fig. 2f). Hexahydrite, paracoquimbite, pickeringite and starkeyite are the dominant minerals. Minor copiapite, coquimbite, tamarugite, halotrichite and gypsum were also identified (Fig. 4c, d).

AMD neutralisation tests

Quality characteristics of untreated pit-lake water samples

The initial water chemistry of open-pit lakes in both study areas is indicative of the acidic and oxidizing conditions prevailing in AMD environments. The measured values of physicochemical and elemental concentrations between the collected samples at each lake, show no significant variation and are in general agreement with those reported in the earlier EU-LIFE project (Charalambides *et al.* 1998). Dissolved oxygen varies from 85% to 90% and pH is 2.8 and 2.5 for Mathiatis and Sha, respectively. However, the water samples of the Sha pit-lake are significantly enriched in sulphate (mean of 37,025 mg/L, whereas the mean value for Mathiatis is 4,764 mg/L) with an estimated 7-fold increase in concentration compared with the Mathiatis pit-lake. Additionally, all elemental concentrations including those of potentially toxic elements are higher in Sha water samples (Table 5). An evaluation of the quality of pit-lake water based on the Ficklin diagram (Ficklin *et al.* 1992; Plumlee *et al.* 1999) indicates a “high-acid high-metal” environment for the Mathiatis pit-lake and an “extreme-metal high-acid” environment for the Sha pit-lake (Fig. 5).

The chemical composition of the untreated water samples demonstrates the significant impact of dissolution of ore minerals as well as the host lavas on pit-lake water quality. Elements such as Cl, Al, B, Ca, K, Mg, Na, Sr are related to the dissolution of silicate minerals, while SO_4^{2-} , Fe, Ag, As, Cd, Co, Cu, Pb, Zn to the oxidation of sulphide minerals. The Mathiatis pit-lake chemistry displays a greater influence of lava host rock-derived elements in contrast with the Sha pit-lake, whereas the concentrations of most metals and SO_4^{2-} are higher. Boron concentration in the Mathiatis water ranges from 4 to 5 mg/L, close to the mean concentration of sea water of 5 mg/L (Cyril 2007), whereas in Sha the concentration is less than 0.4 mg/L.

Effect of neutralisation treatment on the physicochemical parameters of water

The effectiveness of the materials used as neutralisation agents was initially assessed by comparing the physicochemical characteristics of pit-lake water before and after interaction. The results of pH and TDS concentration change, after one and six hours of reaction with the limestone materials, are presented graphically in Fig. 6. Values of neutral or near-neutral pH (>6) were achieved within the first hour in all cases except for Latouros-300 μm in Sha water for which pH did not exceed a pH of 5 even after 6 hours of reaction. It is noted that this specific material is rich in dolomite and Mg-calcite, probably affecting its performance in buffering the pH. Given that dolomite has lower reactivity than calcite (Lottermoser 2010), a lower rate of reaction is expected for this material. Furthermore, pH 5 is approximately the value buffered by Al-OH precipitation, possibly resulting from the incongruent dissolution of silicate minerals in the Latouros sample. Among the neutralisation agents, Mitsero $<150 \mu\text{m}$ yielded the best results in both study areas; pH increased from 2.8 to 7.1 and from 2.5 to 6.5 for Mathiatis and Sha water, respectively, after the first hour of reaction without any significant increase with time thereafter.

TDS concentrations did not change significantly after reaction with any of the treatment materials at both sites, reflecting the conservative character of SO_4^{2-} that remained high ($>4,370 \text{ mg/L}$ in Mathiatis water and $>18,000 \text{ mg/L}$ in Sha water) in all solutions after reaction. It is noted that all neutralisation agents are less effective with Sha samples. The final pH values of treated lake water from this mine ranged from 4.5 to 7.0 and the sulphate concentration dropped by 30% varying from 17,900 to 24,550 mg/L .

Neutralisation by quicklime was more effective than limestone treatment. Initial experimentation showed that the required quantity of quicklime had to be drastically reduced in order to sustain a neutral pH. A second order equation fits well ($R^2 > 0.9$) the experimental data of pH change with varying quicklime concentration for both studied sites (Fig. 7a, b). A concentration of 0.07 g/L for Mathiatis water and 2.75 g/L for Sha has been selected accordingly and used in further experiments

in order to test the effect of reaction time on pH and SO_4^{2-} concentration (Table 6). The pH changed rapidly within the first hour and reached the value of 7.9 for Mathiatis and 9.5 for Sha after 6 hours of reaction (Fig. 7c). Sulphate concentration also shows an abrupt reduction within the first hour of reaction, especially in the instance of Sha water, but without dropping sufficiently to meet water quality recommendations of approximately 500 mg/L (Bowell 2004). SEM-EDS examination of residual grains collected after 6 hours reaction with Sha water revealed that armoured coatings incorporating Ca, S, Mg and Al form on the surface, as well as fill microfissures in the grains (Fig. 8). Also, platy and elongated gypsum crystals are observed in abundance in the residual material indicating that the solution reached gypsum saturation conditions within the reaction period.

Reduction of trace element concentrations in water and comparison of the results with legislation limits

The removal percentage of trace elements at the end of the 6 hours reaction varied for each element and each neutralisation agent as shown in Table 7. The presented results concern the best combination of grain-size and material-mixing concentration. The elements with the highest removal percentage are Cu ($\approx 99\%$), Fe ($\approx 99\%$), Zn (93%) while Cd, Co, Mn and Ni had a removal rate of 60% on average. The results are assessed according to various regulatory limits with respect to different water uses. Specifically, the Greek regulation (Greek Common Ministerial Order 2001) on water quality for human consumption, in compliance with the European Council (EC) (1998) and the US-EPA 2018 Edition of the Drinking Water Standards and Health Advisories Tables (US EPA 2018) were used as drinking water limits, while the Dutch Guide Values and Quality Standards for Assessing Soil and Water Contamination by Heavy Metals (Swartjes 1999) and the Greek Ministerial Order (2009; 2011) were used for irrigation water.

Although the neutralisation test achieved a significant reduction in their concentration, some elements are still above regulation limits (Table 6). After the neutralisation procedures, Cd concentration decreased from 0.04 mg/L to 0.02 mg/L on most samples except Mitsero and Kaos, where the concentration achieved the irrigation limits. Chromium concentration (0.05 mg/L) was

already below the limits in the initial sample. Cobalt follows the same pattern as Cd, with initial concentration of 0.4 mg/L and final from 0.16 to 0.28 mg/L, while the minimum threshold is 0.05 mg/L, either for drinking or irrigation water. Copper has an initial concentration of 3.82 mg/L and after treatment has a concentration of 0.03 to 0.04 mg/L. Iron also had increased removal rates with a 46.2 mg/L starting concentration and an ≈ 0.1 mg/L final concentration. The concentration limits for iron in drinking and irrigation water do not exceed 0.2 mg/L. The limits for manganese and nickel were not achieved after treatment, Mn had an initial concentration of 14.12 mg/L and the lowest concentration achieved was 4.28 ppm while the limit was 0.2 mg/L. Nickel had the lowest removal rate (43%): the initial concentration was 0.16 and the best result from the tests was at 0.06 mg/L, while the limit for drinking water is 0.02 mg/L. Zinc had the second largest concentration in the samples (33.3 mg/L), reaching after the neutralisation processes values from 0.53 to 2.86 mg/L, while the limit varies from 2 to 5 mg/L, leaving some samples off limits.

Discussion

Environmental implications of AMD

Each year the global mining industry produces several billion tonnes of solid inorganic wastes and liquid wastes through its mineral processing and metal production operations (Charbonier 2001; Akcil & Koldas 2006). In the last decades attention has been paid to the environmental issues developed by the mining activities due to big quantities of solid and liquid wastes being produced through exploitation, mineral processing and metal production operations (Plumlee 1999; Lottermoser 2010).

The Mathiatis and Sha mines are among the legacies of the past, when environmental impacts of mining activities were not fully investigated or regulated. Thus, an understanding of the mineralogy and chemistry of waste material and the geochemical processes related to the observed drainage at mine sites, can provide insights for their remediation along with awareness for future environmental issues concerning exploitation of pyrite-rich ores, especially of the VMS type. Typical examples are

the ophiolite related ores in Troodos in Cyprus (e.g., Limni, Kalavassos, Agrokipia, Kokkinopezoula, Apliki) (Constantinou 1980), Caledonides (Løkken, Scorovas, Svano) (Banks *et al.* 1997), Arinteiro and Fornás in Spain (Marina *et al.* 1987), as well as the gigantic pyritic ores of the Iberian Pyrite Belt (IPB) hosted in a volcano-sedimentary sequence (Soriano & Marti 1999; Leblanc *et al.* 2000). Mining activities in those areas have exploited near-surface and outcropping pyritic orebodies, leaving pyrite-rich mine waste, with concomitant generation of acid mine drainage waters, with pH values ranging from 1.5 to 3 (Banks *et al.* 1997; Sánchez España *et al.* 2008; Cohen *et al.* 2011).

A comparison of the Mathiatis physicochemical attributes with other acidic pit-lakes and AMD from Cyprus, the IPB and the Caledonides displays similar values for the pH, sulphate and metal load (Table 5). Sha pit-lake, on the other hand, has significantly higher iron and sulphate content even though the pH has analogous values with the other sites. The similarity of the two studied pit-lakes with the chemistry of IPB pit-lakes as presented by Sánchez-España *et al.* (2008) is shown on the Ficklin classification diagram (Fig. 5). A lower pH value may result in a higher concentration of certain trace elements, a fact that can be noted for the Mathiatis and Sha as well.

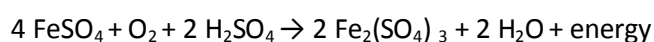
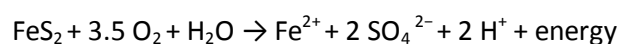
Acid mine drainage and associated weathering products commonly result not only in physical and chemical, but also in biological impairment of surface water, to the point that surrounding areas become devoid of aquatic life. The toll on fish populations has been immense in AMD impacted areas especially after rainstorm events (Nordstrom 2011). Research concerning bioavailability of metals in two fish species in the IPB suggested dependence on the different behaviour of these species (Vicente-Martorell *et al.* 2009), indicating the importance of thorough ecological studies in such areas. In the case of Mathiatis and Sha, situated in a typical arid environment, the impact on the fauna and flora has not been investigated. Further research is needed for the evaluation of adverse effects on biota and changes in the ecosystem due to AMD.

Source of AMD

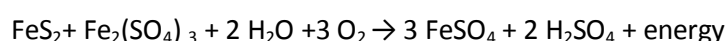
The mineralogy of the mine waste and host rock is a fundamental element for generation of AMD. When exposed to atmospheric conditions, pyrite and chalcopyrite, which are the predominant

ore minerals, are subject to weathering through oxidation. Pyrite oxidation is accomplished by abiotic or biotic indirect oxidation (Lottermoser 2010). The reactions of pyrite and chalcopyrite are as follows:

a) indirect pyrite oxidation (Evangelou 1995; Evangelou & Zhang 1995; Keith & Vaughan 2000):



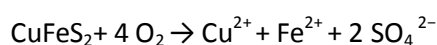
or



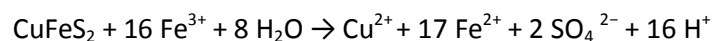
or



b) chalcopyrite oxidation (Costello 2003; Kimball *et al.* 2009):



and

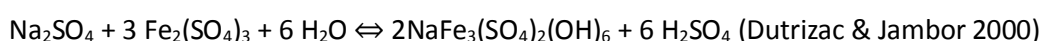


The runoff water then becomes enriched in trace elements contained in the ore minerals (e.g., Co, Cu, Zn, Mn, Ni, As, Se from pyrite, Bullock *et al.* 2017; Grant *et al.* 2018). Dissolved elements and sulphate from weathering processes can remain in solution or form in situ efflorescence minerals (Fig. 3c, d), depending on the local chemical and physical conditions. Hudson – Edwards and Edwards (2005) proved that efflorescent salts in the Mathiatis mine waste facility absorb a high fraction of As, Cu and Zn from the runoff, although they can easily release it back to the environment. The mineral phases bearing the heavy metals are usually the Fe sulphates while Al and Mg phases are not receptive.

When basalt fragments interact with acid solutions, the solubility of alkali and alkaline earth metals increases (Gudbrandsson *et al.* 2008), hence they are released to the environment.

Dissolution of the rock-forming minerals of the basalt provides a natural source of calcium and magnesium in the runoff and a natural neutralisation agent for the acid mine drainage by the binding of SO_4^{2-} through the formation of gypsum and Mg-sulphates. Boron in acid mine waters derives from the basaltic lavas. According to Yamaoka *et al.* (2015), average boron concentration in the Troodos lavas is around 63 mg/kg.

As stated by Nordstrom (2011) pyrite oxidation is a strongly exothermic reaction. The heat produced increases the evaporation rate of mine waters and promotes the formation of efflorescent salts. Reactions such as the creation of natrojarosite



take place on the mine waste resulting in the formation of an ochreous efflorescent crust. At both the Mathiatis and the Sha mines magnesium sulphates predominate in the efflorescence fields, mixed with other secondary minerals, mainly gypsum and Mg-Al sulphates, with limited occurrence of iron sulphates in the lakeshores (Table 4). Those solid soluble salts store acidity and metals until rainstorms flush them out (Jambor *et al.* 2000).

Pit-lake water geochemistry

The chemical analysis of the water samples demonstrates the significant impact of the dissolution of ore minerals, as well as the host lavas on the geochemistry of the pit-lake water. Elements such as Al, B, Ca, Cl, K, Mg, Na, Sr are related to the dissolution of rock forming minerals, while SO_4^{2-} , Cu, Fe, As, Cd, Co, Pb and Zn to the oxidation of ore minerals. The Mathiatis pit-lake water chemistry displays a greater influence of lava-derived elements in comparison to the Sha pit-lake water. This is evident by the lower Fe, Cu, Zn, Pb, Mn, Co and As metal load at Mathiatis, relative to the Sha pit-lake. A remarkable difference is detected especially in the concentration of SO_4^{2-} in the Sha pit-lake water (mean 37,025 mg/L) as compared with the Mathiatis pit-lake water (mean 4,764 mg/L). A

reasonable explanation is that at Mathiatis AMD is generated as a result of the oxidation of low-grade disseminated to semi-massive pyrite mineralisation, exposed on the walls of the open pit, as well as of weathering of minor disseminated pyrite in the country rock and the mine waste (Fig. 9). At Sha, AMD is produced by oxidation of the massive Cu-pyrite ore body exposed to weathering; hence, the metal load of the Sha lake water is heavier than that of the Mathiatis pit-lake. The higher extent and depth of the pit-lake of Mathiatis accounts also for the lower metal concentrations in water as compared to the Sha, due to metal dilution.

Periodic pit-lake water monitoring data, especially on seasonal chemical variations of pit-lake waters in comparison with the mineralogy of efflorescence formed during dry periods, are lacking. In spite of this, it is reasonable to expect that dissolution of sulphates following rainfall events might have a detectable geochemical response. Dissolution of metal and alkali hydrous-sulphates during storm runoff events has been found to increase concentrations of dissolved metals and SO_4^{2-} in surface waters elsewhere (e.g., Harris *et al.* 2003, Hammarstrom *et al.* 2005). Evaporative precipitation of hydrous alkali- and metal-sulphate efflorescence might take place during dry periods on the lakeshore at Mathiatis and Sha. The predominance of magnesium sulphates in efflorescence is due to their high resistance to dissolution, since Mg salts remain in the environment longer than Fe salts (Jambor *et al.* 2000; Chipera & Vaniman, 2007). Pickeringite is the predominant aluminum sulphate salt in the samples of the mine waste. Because of the low pH needed for the dissolution of the basaltic lavas, aluminum sulphate salts tend to form later than magnesium sulphates, in line with observations by Blowes *et al.* (2003). Gypsum is ubiquitous at all sites in the open pits making it the most common supergene mineral. This is a result of high Ca and SO_4^{2-} concentrations in acidic water and the lower solubility of the mineral than any other sulphate.

Effectiveness of neutralisation agents tested

The noted differences in the effectiveness of the neutralisation agents for the two studied pit-lakes are attributed to differences in water chemistry of the two sites and underline the significance of site-specific conditions on the choice of the most appropriate neutralisation method (Bowell

2004). In general, limestone materials did not achieve removal of sulphates to levels lower than the maximum allowed limit in irrigating water. Similar results were produced by Potgieter – Vermaak *et al.* (2006) in neutralisation tests with fabricated acid mine drainage. A possible explanation lies in the fact that the neutralisation potential is correlated with Fe concentration in the solution. As described by Maree *et al.* (1992), when mixing carbonate agents and AMD with high Fe concentrations, an impenetrable crust of Fe-hydroxides is created. This crust armours a portion of the agent not allowing it to react any further. The identification of encrusted grains by SEM-EDS (Fig. 8) even for the quicklime treatment in the present research, indicates that armouring is taking place during reaction with the rich in Fe solution. Specifically, unreacted grains appear to be covered by a crust containing gypsum crystals and rich in Mg and Al phases. During their experiments with limestone Hammarstrom *et al.* (2003) observed the precipitation of aluminous material in near-surface calcite micropores. They suggested that a gradient in pH exists from the bulk value in solution, to an elevated value near the dissolving limestone surface, explaining the occurrence of an Al phase near the limestone surface, where pH is likely to reach a value of 5 or higher during the early stages of the experiment. Furthermore, Ineich *et al.* (2017) in experiments of magnesium sulphate precipitation with lime have observed precipitate coating effects, leading to the occlusion of unreacted $\text{Ca}(\text{OH})_2$ particles. Research performed by Skousen *et al.* (2000) indicated that by adding sodium in the form of soda ash and caustic soda (Na_2CO_3 and NaOH) along with the neutralisation agent can reduce the armouring effect and effectively remove Mn from the solution. However, health and safety issues, poor sludge settling rates and potential sodium toxicity along with highest cost of all chemicals, limit the applicability of such substances during active AMD treatment (Trumm 2010).

The increase of pH to alkaline levels resulted in the precipitation of most of the elements as hydro-oxides and sulphates, leading to a decrease of their concentration in the solution. Mn removal is more challenging due to its complex chemistry and the fact that a pH of ca. 9 is required for it to precipitate. For example, the Mn^{2+} is relatively soluble at pH 8, while above that value it can precipitate either as MnCO_3 or as $\text{Mn}(\text{OH})_2$ if CO_2 is low in the solution (Rose *et al.* 2003). In order to

remove Mn from the solution a different approach should be followed, such as the use of activated carbon (Mondal *et al.* 2007; Emmanuel & Veerabhadra Rao 2009).

The removal of sulphates from the solution also did not reach the legislation limits, for both study areas. Regarding Mathiatis, the effect of either lime or limestone did not produce any significant reduction in sulphate concentration, whereas in the Sha samples sulphate concentration has been reduced by approximately 95%. However, it is noted that in Mathiatis epilimnion, sulphate concentration (4,764 mg/l) is much lower than Sha (37025 mg/l), indicating oversaturated conditions in the latter. Based on the quantity of quicklime added and assuming initial gypsum saturation, the experimental results are in agreement with theoretical calculations of SO_4^{2-} removal by gypsum precipitation, i.e., 0.01 mol/L and 0.04 mol/L for Mathiatis and Sha, respectively. Experimental results indicate that, reaction with lime or limestone can be considered as a pre-treatment method as far as sulphate removal is concerned, and a secondary treatment method would be necessary such as electrocoagulation or filtration as described by Ashane *et al.* (2018).

Conclusions

The Mathiatis and Sha deposits -classified within the Cyprus-type VMS class- are composed mainly of pyrite, marcasite and minor chalcopyrite, and have typical gold grades for this type of deposits.

The mine waste kept in the Mathiatis storage facility has paste pH values of 2.2 to 4.7 and negative NNP indicating an acid generation potential. Also, elevated As and Cu concentrations due to the presence of ore minerals exceed the average topsoil values of Cyprus and the Dutch intervention limits.

A wide spectrum of efflorescent salts was identified at the lakeshore of the Mathiatis and Sha open pits, with the strongest presence being accredited to gypsum, hexahydrate and starkeyite for Mathiatis and hexahydrate, paracoquimbite, pickeringite and starkeyite for Sha respectively.

The oxidation of sulphides along with the dissolution of silicate minerals, contained in the Mathiatis mine waste, generate AMD feeding the acid pit-lake. Weathering products rich in Ca-Mg-Fe sulphates are also being formed in situ during the process. An extensive efflorescence field, bearing Mg-Fe mineral phases, was present near the Mathiatis mine waste facility due to saturation and precipitation of the surface AMD runoff. These efflorescent salts release acidity and metals during flush out events induced by rainstorms feeding the pit-lake. A close relation between the chemistry of the efflorescent salts and the chemical composition of the pit-lake water has been observed.

An evaluation of the quality of the pit-lake water for the Mathiatis and Sha indicated a “high-acid high-metal” environment for the Mathiatis pit-lake and an “extreme-metal high-acid” environment for the Sha. Lava derived elements are enriched in the Mathiatis pit-lake water in contrast with the Sha pit-lake, where the presence of most metals and SO_4^{2-} is stronger.

The laboratory scale experiments involving low-cost local limestone byproducts as neutralisation agents to treat the water, achieved neutral pH values of ca. 7 and reduced most of the heavy metal concentrations by 60% to 95%. Although the use of local limestone byproducts is not sufficient for full remediation, due to low efficiency in neutralisation and continued presence of Mn and SO_4^{2-} , it could be used as a low-cost pretreatment method for AMD.

Acknowledgments

This study was partially funded by the Special Account for Research Grants, NKUA to N.S. and A.A (Kapodistrias Program). The authors are deeply grateful to Dr. Eleni Georgiou-Morisseau, former Director of the Geological Survey Department of Cyprus, and Dr. Andreas Zissimos, for discussions and making allowable storage and partial analysis of water samples in the Chemical laboratory. Guiding in the Troodos ophiolite by Georgios Hadjigeorgiou (MSc), senior geologist of the Geological Survey Department of Cyprus, is kindly acknowledged. The authors would like to thank Dr. George

Maliotis, former Director General of HCM, for permits to work in the abandoned mines, for guiding in mining sites of the Troodos, helpful discussions on local geology and hospitality when in Cyprus. Tasos Sotiropoulos and Theano Stavrou are thanked for field assistance. The help by Evangelos Michailidis (NKUA) and Dr. George Economou (Institute of Geology and Mineral Exploration) with SEM work is kindly acknowledged. We acknowledge the thorough reviews and constructive comments on the manuscript by the Chief Editor of GEEA Scott Wood, as well as Richard Preece and Liam Bullock that greatly improved the quality of the paper.

References

- Adamides, N.G. 1980. The form and environment of formation of the Kalavassos ore deposits, Cyprus. *In: Panayiotou, A. (ed) Ophiolites: Proceedings, International Ophiolite Symposium*. Cyprus 1979. Cyprus Geological Survey, 117-127.
- Akcil, A. & Koldas, S. 2006. Acid mine drainage (AMD): causes, treatment and case studies. *Journal of Cleaner Products*, **14**, 1139–1145.
- Antivachis, D., Chatzitheodoridis, E., Skarpelis, N. & Komnitsas, K. 2017. Secondary sulphate minerals in a Cyprus type ore deposit, Apliki, Cyprus: Mineralogy and its implications regarding the chemistry of pit lake water. *Mine Water and the Environment*, **36**, 2, 226-238, <https://doi.org/10.1007/s10230-016-0398-0>
- Ashane, W., Fernando, M., Ilankoon, I.M.S.K., Syed, T. & Yellishetty, M. 2018. Challenges and opportunities in the removal of sulphate ions in contaminated mine water: A review. *Minerals Engineering*, **117**, 74-90, <https://doi.org/10.1016/j.mineng.2017.12.004>
- Banks, D., Younger, P.L., Arnesen, R.T., Iversen, E.G. & Banks, S.B. 1997. Mine-water chemistry: the good, the bad and the ugly. *Environmental Geology*, **32**, 3, 157-174.
- Bear, L.M. 1963. The mineral resources and mining industry of Cyprus. *Cyprus Geological Survey Bulletin*, **1**, 224.
- Blowes, D. W., Ptacek, C. J., Jambor, J. L. & Weisener, C. G. 2003. The geochemistry of acid mine drainage, *Environmental Geochemistry*, **9**, 149-204.
- Bowell, R. J. 2004. A review of sulphate removal options for mine waters. *In: Jarvis, A. P., Dudgeon, B. A. & Younger, P. L. (eds) Mine Water 2004 – Proceedings International Mine Water Association Symposium 2*. Newcastle upon Tyne, United Kingdom, 75-91.
- Bullock, L.A., Parnell, J., Perez, M., Feldmann, J. & Armstrong, J.G. 2017. Selenium and other trace element mobility in waste products and weathered sediments at Parys Mountain Copper Mine, Anglesey, UK. *Minerals*, **7**, 229. Doi:10.3390/min7110229

Changul, C., Sutthirat, C., Padmanahban, G. & Tongcumpou, C. 2010. Chemical characteristics and acid drainage assessment of mine tailings from Akara Gold mine in Thailand. *Environmental Earth Sciences*, **60**, 1583-1595, doi: 10.1007/s12665-009-0293-0

Charbonier, B. 2001. *Management of Mining, Quarrying and Ore-processing Waste in the European Union*. Bureau de Recherches Gèologiques et Minières, European Union, **75**.

Charalambides, A., Baker, J., Constantinou, C.A., Constantinou, G., Kyriacou, E., Van Dijk, P., Gournari, G., Van Os, B. & Shiathas, A. 1997. Surface and groundwater pollution from old mines in Cyprus. In: Soulios, G. (ed) *Proceedings of the Fourth Hydrogeological Conference*, Thessaloniki, Greece, 570–581.

Charalambides, A., Kyriacou, E., Constantinou, C., Baker, J., van Os, B., Gurnari, G., Shiathas, A., van Dijk, P. & van der Meer, F. 1998. *Mining Waste Management on Cyprus: Assessment, Strategy Development and Implementation*. Geological Survey Department, Nicosia.

Charalambides, A., Petrides, G. & Pashalidis, I. 2003. Rainwater characteristics over an old sulphide mine refuse in Sha, Cyprus. *Atmospheric Environment*, **37**, 1921-1926.

Chipera, S.J. & Vaniman, D.T. 2007. Experimental stability of magnesium sulfate hydrates that may be present on Mars. *Geochimica et Cosmochimica Acta*, **71**, 1, 241-250.

Chou, I.-M., Seal II, R.R. & Wang, A. 2013. The stability of sulfate and hydrated sulfate minerals near ambient conditions and their significance in environmental and planetary sciences. *Journal of Asian Earth Sciences*, **62**, 734-758.

Cohen, D.R., Rutherford, N.F., Morisseau, E. & Zissimos, A.M. 2011. *Geochemical Atlas of Cyprus*. Sydney, UNSW Press.

Cohen, D.R., Rutherford, N.F., Morisseau, E. & Zissimos, A.M. 2012. Geochemical patterns in the soils of Cyprus. *Science of the Total Environment*, **420**, 250-262.

Constantinou, G. 1980. Metallogenesis associated with the Troodos ophiolite. In: Panayiotou, A. (ed) *Ophiolites: Proceedings, International Ophiolite Symposium*, 1979. Geological Survey Department, Nicosia, Cyprus, 663-674.

Constantinou, G. & Govett, G.J.S. 1973. Geology, geochemistry, and genesis of Cyprus sulfide deposits. *Economic Geology*, **68**, 843–858.

Costello, C. 2003. *Acid mine drainage: innovative treatment technologies. National network of environmental management studies fellow*. U.S.E.P.A., Office of Solid Waste and Emergency Response, Washington D.C., **47**.

Cyprus Geological Survey. 2007. *Mineral Resources Map of Cyprus*. Scale 1:250.000. Geological Survey Department, Nicosia, Cyprus.

Cyril, J. 2007. Seawater desalination: Boron removal by ion exchange technology. *Desalination*, **205**, 47-52.

Dutrizac, J.E. & Jambor, J.L. 2000. Jarosites and their application in hydrometallurgy. *In*: Alpers, C.N., Jambor, J.L. & Nordstrom, D.K. (eds) Sulfate Minerals: Crystallography, Geochemistry, and Environmental Significance, *Reviews in Mineralogy and Geochemistry*, Mineralogical Society of America, Chantilly, Virginia, **40**, 405-452.

Emmanuel, K.A. & Veerabhadra Rao, A. 2009. Comparative study on adsorption of Mn(II) from aqueous solution on various activated carbons. *E-Journal of Chemistry*, **6**, 693-704.

Equeenuddin, M.S., Tripathy, S., Sahoo, P.K. & Panigrahi, M.K. 2010. Hydrogeochemical characteristics of acid mine drainage and water pollution at Makum Coalfield, India. *Journal of Geochemical Exploration*, **105**, 75–82.

European Council. 1998. Drinking Water Directive. *Council Directive 98/83/EC of 3 November 1998 on the quality of water intended for human consumption*. Official Journal **L 330**, 05/12/1998, 32-54, European Union.

Evangelou, V.P. 1995. *Pyrite oxidation and its control*. CRC Press, Boca Raton, **293**.

Evangelou, V.P. & Zhang, Y.L. 1995. A review: pyrite oxidation mechanisms and acid mine drainage prevention. *Critical Reviews in Environmental Science and Technology*, **25**, 141–199.

Favas, P.J.C., Pratas, J. & Gomes, M.E.P. 2012. Hydrochemistry of superficial waters in the Adoria mine area (Northern Portugal): environmental implications. *Environmental Earth Sciences*, **65**, 363-372.

Favas, P.J.C., Sarkar, S.K., Rakshit, D., Venkatachalam, P. & Prasad, M.N.V. 2016. Acid Mine Drainages from Abandoned Mines: Hydrochemistry, Environmental Impact, Resource Recovery, and Prevention of Pollution. *In*: Prasad, M.N.V. & Shih, K. (eds) *Environmental Materials and Waste, Resource Recovery and Pollution Prevention*, Academic Press, 413-462.

Ficklin, W.H., Plumlee, G.S., Smith, K.S. & McHugh, J.B. 1992. Geochemical classification of mine drainages and natural drainages in mineralized areas. *In*: Kharaka, Y.K. & Maest, A.S. (eds) *Water-rock interaction: Seventh International Symposium on Water-Rock Interaction*, Park City, Utah, 381-384.

Follows, E. 1992. Patterns of reef sedimentation and diagenesis in the Miocene of Cyprus. *Sedimentary Geology*, **79**, 1-4, 225-253.

Gale, N.H. & Stos-Gale, Z.A. 1986. Oxhide copper ingots in Crete and Cyprus and the Bronze Age Metals Trade. *The Annual of the British School at Athens*, **81**, 81-100.

Grande, J. A., Valente, T., de la Torre, M. L., Santisteban, M., Cerón, J.C. & Pérez-Ostalé, E. 2014. Characterization of acid mine drainage sources in the Iberian Pyrite Belt: base methodology for quantifying affected areas and for environmental management. *Environmental Earth Sciences*, **71**, 2729-2738.

Grant, H., Hannington, M., Petersen, S., Frische, M. & Fuchs, S. 2018. Constraints on the behavior of trace elements in the actively-forming TAG deposit, Mid-Atlantic Ridge, based on LA-ICP-MS analyses of pyrite. *Chemical Geology*, **498**, 45-71, <https://doi.org/10.1016/j.chemgeo.2018.08.019>

Gray, N. 1997. Environmental impact and remediation of acid mine drainage: a management problem. *Environmental Geology*, **30**, 62-71.

Greek Common Ministerial Order. 2001. K.Y.A Y2/2600/2001. *FEK (Official Gazette)* 892/11-07-2001.

Greek Ministerial Order. 2009. Y.A. 39626/2208/E130/2009. *FEK (Official Gazette)* 2075/25-09-2009.

Greek Ministerial Order. 2011. Y.A. 1811/2208. *FEK (Official Gazette)* 3322/30-12-2011.

Gudbrandsson, S., Wolff-Boenisch, D., Gislason, S. & Oelkers, E.H. 2008. Dissolution rates of crystalline basalt at pH 4 and 10 and 25–75°C. *Mineralogical Magazine* **72**(1), 155-158.

Hadjistavrinou, Y. & Constantinou, G. 1982. Cyprus. *In*: Dunning, F.W., Mykura, W., & Slater, D. (eds) *Mineral Deposits of Europe, Southeast Europe*. The Mineralogical Society, Great Britain, **2**, 255-277.

Hammarstrom, J.M., Seal II, R.R., Meier, A.L. & Kornfeld, J.M. 2005. Secondary sulfate minerals associated with acid drainage in the eastern US: recycling of metals and acidity in surficial environments. *Chemical Geology*, **215**, 407–431.

Hammarstrom, J. M., Sibrell, P.L. & Belkin, H.E. 2003. Characterization of limestone reacted with acid-mine drainage in a pulsed limestone bed treatment system at the Friendship Hill National Historical Site, Pennsylvania, USA. *Applied Geochemistry*, **18**, 1705-1721.

Hannington, M.D., Galley, A.G., Herzig, P.M. & Petersen, S. 1998. Comparison of the TAG mound and stockwork complex with Cyprus-type massive sulfide deposits. *In*: Herzig, P.M., Humphris, S.E., Miller, D.J. & Zierenberg, R.A. (eds) *Proceedings of the Ocean Drilling Program, Scientific Results*, **158**, 389-415.

Hannington, M.D., Herzig, P.M., Scott, S.D., Thompson, G. & Rona, P.A. 1991. Comparative mineralogy and geochemistry of gold-bearing sulfide deposits on the mid-ocean ridges. *Marine Geology*, **101**, 217-248.

Harris, D.L., Lottermoser, B.G. & Duchesne, J. 2003. Ephemeral acid mine drainage at the Montalbion silver mine, north Queensland, Australian. *Journal of Earth Sciences*, **50**, 5, 797-809.

Herzig, P.M., Hannington, M.D., Scott, S.D., Maliotis, G., Rona, P.A. & Thompson, G. 1991. Gold-rich sea-floor gossans in the Troodos ophiolite and on the mid-Atlantic ridge. *Economic Geology*, **86**, 1747–1755.

- HMC. 1983. *Geological map of the Sha open pit mine*. Hellenic Mining Company.
- Hudson-Edwards, K.A. & Edwards, S.J. 2005. Mineralogical controls on storage of As, Cu, Pb and Zn at the abandoned Mathiatis massive sulphide mine, Cyprus. *Mineralogical Magazine*, **69**, 695-706.
- Ineich, T., Degreve, C., Karamoutsos, S. & du Pleissis, C. 2017. Utilization efficiency of lime consumption during magnesium sulfate precipitation. *Hydrometallurgy*, **173**, 241-249.
- Jamal, A., Dhar, B.B., Ratan, S. 1991. Acid mine drainage control in an open cast coal mine. *Mine Water and the Environment*, **10**, 1-16.
- Jambor, J.L., Nordstrom, D.K. & Alpers, C.N. 2000. Metal-sulfate salts from sulfide mineral oxidation. In: Alpers, C.N., Jambor, J.L. & Nordstrom, D.K. (eds) *Sulfate Minerals: Crystallography, Geochemistry, and Environmental Significance. Reviews in Mineralogy and Geochemistry*, **40**, 303-350.
- Kassianidou, V. 2013. Mining Landscapes of Prehistoric Cyprus. *Metalla*, **20**, 2, 5-57.
- Kaur, G., Couperthwaite, S., Hatton-Jones, B. & Millar, G. 2018. Alternative neutralisation materials for acid mine drainage treatment. *Journal of Water Process Engineering*, **22**, 46-58.
- Keith, C.N. & Vaughan, D.J. 2000. Mechanisms and rates of sulphide oxidation in relation to the problems of acid rock (mine) drainage. In: Cotter-Howells, J.D., Campbell, L.S., Valsami-Jones, E. & Batchelder, M. (eds) *Environmental Mineralogy: Microbial Interactions, Anthropogenic Influences, Contaminated Land and Waste Management*. Mineralogical Society Special Publication, London, UK.
- Kelly, M. 1991. *Mining and the Freshwater Environment*. 2nd ed. Elsevier Science Publishers Ltd, London, New York, **231**.
- Kimball, B. E., Mathur, R., Dohnalkova, A. C., Wall, A. J., Runkel, R. L. & Brantley, S. L., 2009. Copper isotope fractionation in acid mine drainage. *Geochimica et Cosmochimica Acta*, **73**, 1247–1263.
- Knapp, A.B., Kassianidou, V. & Donnelly, M. 2001. Copper Smelting in Late Bronze Age Cyprus: The excavation at Politiko Phorades. *Near Eastern Archeology*, **64**, 204-210.

Lavender, D. 1962. *The story of Cyprus Mines Corporation*. Huntington Library publications, San Marino, California, **387**.

Leblanc, M., Morales, J.A., Borrego, J. & Elbaz-Poulichet, F. 2000. 4500-year-old mining pollution in Southwestern Spain: Long-Term implications for modern mining pollution. *Economic Geology*, **95**, 3, 655-662.

Lei, L., Song, C., Xie, X., Li, Y. & Wang, F. 2010. Acid mine drainage and heavy metal contamination in groundwater of metal sulfide mine at arid territory (BS mine, Western Australia). *Transactions of Nonferrous Metals Society of China*, **20**, 8, 1488-1493, [https://doi.org/10.1016/S1003-6326\(09\)60326-5](https://doi.org/10.1016/S1003-6326(09)60326-5)

Li, Y., Qian, G., Li, J. & Gerson, A.R. 2015. Kinetics and roles of solution and surface species of chalcopyrite dissolution at 650 mV. *Geochim. Cosmochim. Acta*, **161**, 188-202.

Lottermoser, B. G. 2010. *Mine Wastes: Characterization, Treatment and Environmental Impacts*. 3rd Edition, Springer-Verlag Berlin Heidelberg, **400**.

Lydon, J.W. 1984. Ore deposit models – 8. Volcanogenic massive sulfide deposits. Part 1: A descriptive model. *Geoscience Canada*, **11**, 195-202.

Lydon, J.W. & Galley, A. 1986. The chemical and mineralogical zonation of the Mathiati alteration pipe, Cyprus, and its genetic significance. In: Gallagher, M.J., Ixer, R.A., Neary, C.R., & Prichard, H.M. (eds) *Metallogeny of basic and ultrabasic rocks*, Institute of Mining and Metallurgy, London, 49-68.

Machemer, S.D. & Wilderman, T.R. 1992. Adsorption compared with sulfide precipitation as metal removal processes from acid mine drainage in a constructed wetland. *Journal of Contaminant Hydrology*, **9**, 115-131.

Maree, J.P., du Plessis, P. & van der Walt, C.J. 1992. Treatment of acidic effluents with limestone instead of lime. *Water Science Technology*, **26**, 345–355.

Marina, E.F., Samper, J. & Guzmán, F.V. 1987. *The Mining Industry in Spain*. Instituto Geológico y Minero de España (I.G.M.E.), Madrid, **181**.

Mondal, P. Balomajumder, C. & Mohanty, B. 2007. A laboratory study for the treatment of arsenic, iron, and manganese bearing ground water using Fe^{3+} impregnated activated carbon: Effects of shaking time, pH and temperature. *Journal of Hazardous Materials*, **144**, 420-426.

Moussoulos, L. 1957. Contribution à l'étude des Gisements de Pyrite cuivreuse de l'île de Chypre. Recherches géologiques et minières dans la région de Kalavassos. *Annales Géologiques des Pays Helléniques*, **1**, 8, 269-320.

Nieva, N.E., Borgnino, L. & García, M.G. 2018. Long term metal release and acid generation in abandoned mine wastes containing metal-sulphides. *Environmental Pollution*, **242**, 264-276, <https://doi.org/10.1016/j.envpol.2018.06.067>

Nieva, N.E., Borgnino, L., Locati, F. & García, M.G. 2016. Mineralogical control on arsenic release during sediment–water interaction in abandoned mine wastes from the Argentina Puna. *Science of the Total Environment*, **550**, 1141-1151.

Ng, S. & Malpas, J. 2013. Impact of Acid Mine Drainage on the hydrogeological system at Sia, Cyprus. *Geophysical Research Abstracts*, **15**, EGU General Assembly, 7-12 April, 2013, Vienna, Austria.

Nordstrom, D.K. 2011. Mine waters: Acidic to circumneutral. *Elements*, **7**, 393-398.

Olias, H., Bell, T.L. & Longaker, J.J. 2004. Seasonal water quality variations in river affected by acid mine drainage: The Odiel river (South west Spain). *Science of Total Environment*, **333**, 267-281.

Oudin E. & Constantinou G. 1984. Black smoker chimney fragments in Cyprus sulphide deposits. *Nature*, **308**, 349–353.

Palamakumbura, R. & Robertson, A. 2018. Pliocene–Pleistocene sedimentary–tectonic development of the Mesaoria (Mesarya) Basin in an incipient, diachronous collisional setting: Facies evidence from the north of Cyprus. *Geological Magazine*, **155**, 997-1022, <https://doi.org/10.1017/S0016756816001072>

Panayiotou, A. 1968. The Sha mine. Geological Survey Department, **2**, Ministry of Commerce and Industries, Republic of Cyprus, 41-56.

Plumlee, G.S. 1999. The environmental geology of mineral deposits. *In*: Plumlee, G.S. & Logsdon, M.J. (eds) *The Environmental Geochemistry of Mineral Deposits, Part A: Processes, Techniques, and Health Issues*. Reviews in Economic Geology, **6A**, 71-116.

Plumlee, G.S., Smith, K.S., Montour, M.R., Ficklin, W.H. & Mosier, E.L. 1999. Geologic controls on the composition of natural waters and mine waters draining diverse mineral deposits. *In*: Filipek, L.H. & Plumlee, G.S. (eds) *The Environmental Geochemistry of Mineral Deposits, Part B, Case Studies and Research Topics*, Reviews in Economic Geology, **6B**, 373-432.

Potgieter-Vermaak, S., Potgieter, J., Monama, P. & Van Grieken, R. 2006. Comparison of limestone, dolomite and fly ash as pre-treatment agents for acid mine drainage. *Minerals Engineering*, **19**, 454-462.

Prichard, H.M. & Maliotis, G. 1998. Gold mineralization associated with low-temperature, off-axis, fluid activity in the Troodos ophiolite, Cyprus. *Journal of the Geological Society*, **155**, 223-231, <https://doi.org/10.1144/gsjgs.155.2.0223>

Rawat, N.S. & Singh, G. 1982. The role of micro-organism in the formation of acid mine drainage in the North Eastern Coal Field of India. *International Journal of Water*, **2**, 29-36.

Robertson, A.H.F. 1975. Cyprus umbers: basalt-sediment relationships on a Mesozoic ocean ridge. *Journal of the Geological Society*, **131**, 5, 511-531.

Romero, A., González, I. & Galán, E. 2011. Stream water geochemistry from mine wastes in Peña de Hierro, Riotinto area, SW Spain: a case of extreme acid mine drainage. *Environmental Earth Sciences*, **62**, 3, 645-656.

Rona, P.A. 2005. TAG hydrothermal field: a key to modern and ancient seafloor hydrothermal VMS ore-forming systems. *Proceedings 8th Biennial SGA Meeting*, Beijing, China, 687-690.

Rose, A.W., Shah, P.J. & Means, B. 2003. Case studies of limestone-bed passive systems for manganese removal from acid mine drainage. *Proceedings Of the American Society of Mining and Reclamation*, Billings, MT, USA.

Rubeska, I., Korecková, J. & Weiss, D. 1977. The determination of gold and palladium in geological materials by atomic absorption after extraction with dibutyl sulphide. *Atomic Absorption Newsletter*, **16**, 1-3.

Sánchez-España, J., López-Pamo, E., Santofimia Pastor, E. & Díez-Ercilla, M. 2008. The acidic mine pit lakes of the Iberian Pyrite Belt: An approach to their physical limnology and hydrogeochemistry. *Applied Geochemistry*, **23**, 1260-1287, DOI:10.1016/j.apgeochem.2007.12.036

Schmiermund, R.L. & Drozd, M.A. 1997. Acid mine drainage and other mining-influenced waters (MIW). In: Marcus, J. (ed.) *Mining Environmental Handbook: Effects of Mining on the Environment and American Environmental Controls on Mining*. Imperial College Press, London, 599-617.

Seal II, R.R. & Shanks III, W.C. 2008. Sulfide oxidation: insights from experimental, theoretical, stable isotope, and predictive studies in the field and laboratory. *Applied Geochemistry*, **23**, 2, 101-342.

Skousen, J.G., Sexstone, A. & Ziemkiewicz, P.F. 2000. Acid mine drainage control and treatment. In: Barnhisel, R.I. (ed) *Reclamation of Drastically Disturbed Lands*. Monograph No. 41, *American Society of Agronomy*, Madison, WI.

Soltani, N., Moore, F., Keshavarzi, B. & Sharifi, R. 2014. Geochemistry of trace metals and rare earth elements in stream water, stream sediments and acid mine drainage from Darrehzar Copper Mine, Kerman, Iran. *Water Quality*, **6**, 97-114.

Soriano, C. & Marti, J. 1999. Facies analysis of volcano-sedimentary successions hosting massive sulfide deposits in the Iberian Pyrite belt, Spain. *Economic Geology*, **94**, 6, 867-882.

Swartjes, F. 1999. Risk-based assessment of soil and groundwater quality in the Netherlands: Standards and remediation urgency. *Risk Analysis*, **19**, 6.

Szczepanska, J. & Twardowska, I. 1999. Distribution and environmental impact of coal-mining wastes in Upper Silesia, Poland. *Environmental Geology*, **38**, 249–258.

Tremblay, G.A. & Hogan, C.M. (eds) 2001. *Mine Environment Neutral Drainage (MEND) Program Volume 4- Prevention and Control*. Canada Centre for Mineral and Energy Technology, Natural Resources Canada, Ottawa.

Trumm, D. 2010. Selection of active and passive treatment systems for AMD flow charts for New Zealand conditions. *New Zealand Journal of Geology and Geophysics*, **53**, 195-210.

US Environmental Protection Agency. 1978. EPA-NERL: 375.4: Sulfate by Turbidity. NEMI. https://www.nemi.gov/methods/method_summary/5316/

US Environmental Protection Agency. 1994. Technical Document: Acid Mine Drainage Prediction. <https://www.epa.gov/sites/production/files/2015-09/documents/amd.pdf>

US Environmental Protection Agency. 1996. Soil and waste pH, Method 9045C, SW-846.

US Environmental Protection Agency, 2018. Edition of the Drinking Water Standards and Health Advisories Tables. EPA 822-F-18-001. Office of Water, U.S. Environmental Protection Agency Washington, DC March 2018

USGS 2010. *Coal-Mine-Drainage Projects in Pennsylvania*. U.S. Department of the Interior, U.S. Geological Survey, <http://pa.water.usgs.gov/projects/energy/amd/index.php>

USGS 2014. 2014 *Minerals Yearbook, Cyprus*. United States Geological Society. December 2017.

Vicente-Martorell, J.J., Galindo-Riaño, M.D., García Vargas, M. & Granado-Castro, M.D. 2009. Bioavailability of heavy metals monitoring water, sediment and fish species from a polluted estuary. *Journal of Hazardous Materials*, **162**, 823–836.

Yamaoka, K., Matsukura, S., Ishikawa, T. & Kawahata, H. 2015. Boron isotope systematics of a fossil hydrothermal system from the Troodos ophiolite, Cyprus: Water–rock interactions in the oceanic crust and subseafloor ore deposits. *Chemical Geology*, **396**, 61-73.

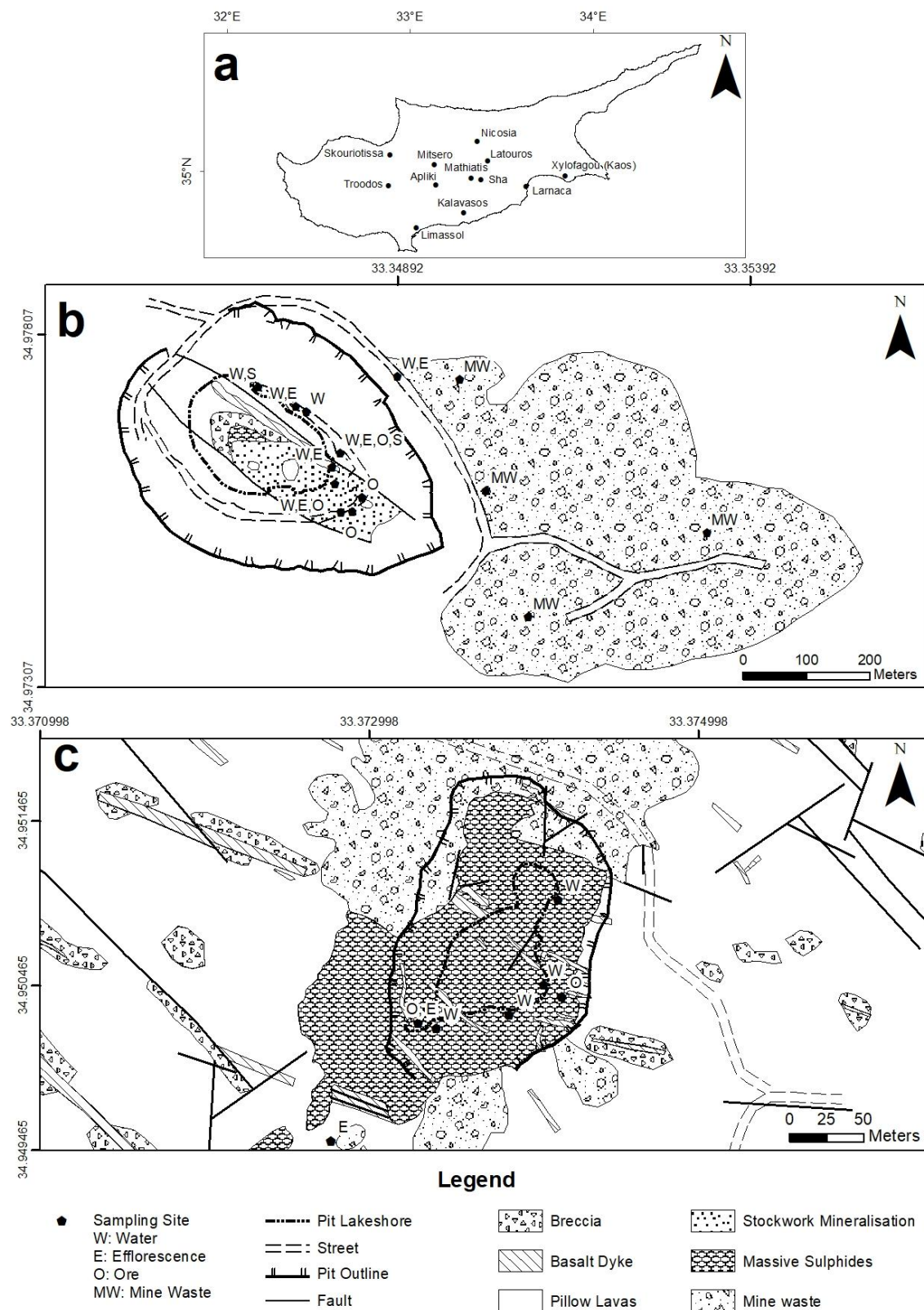


Fig. 1. (a) Map of Cyprus; (b) Geological map of Mathiatis mine (modified after Lydon & Galley 1986; Hannington *et al.* 1998); (c) Geological map of Sha mine (HMC 1983).

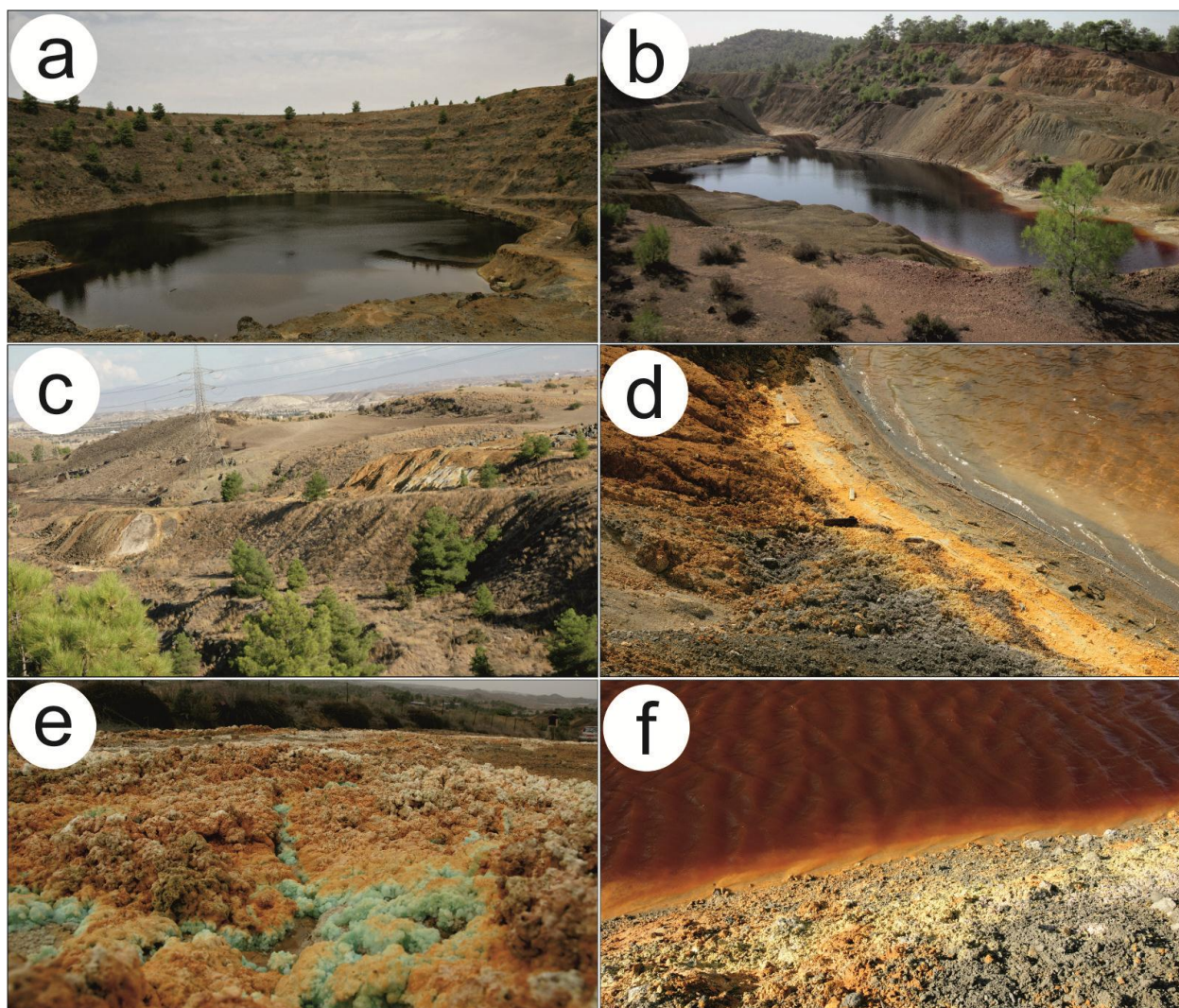


Fig. 2. (a) View of the Mathiatis abandoned mine from the SE; (b) View of the Sha pit-lake from the NNE; (c) The Mathiatis mine waste facility; (d) Efflorescence field on the lakeshore of the Mathiatis open-pit lake; (e) Efflorescence at the Mathiatis mine waste facility; (f) Exposed massive sulphide ore and efflorescence field on the lakeshore of the Sha pit-lake.

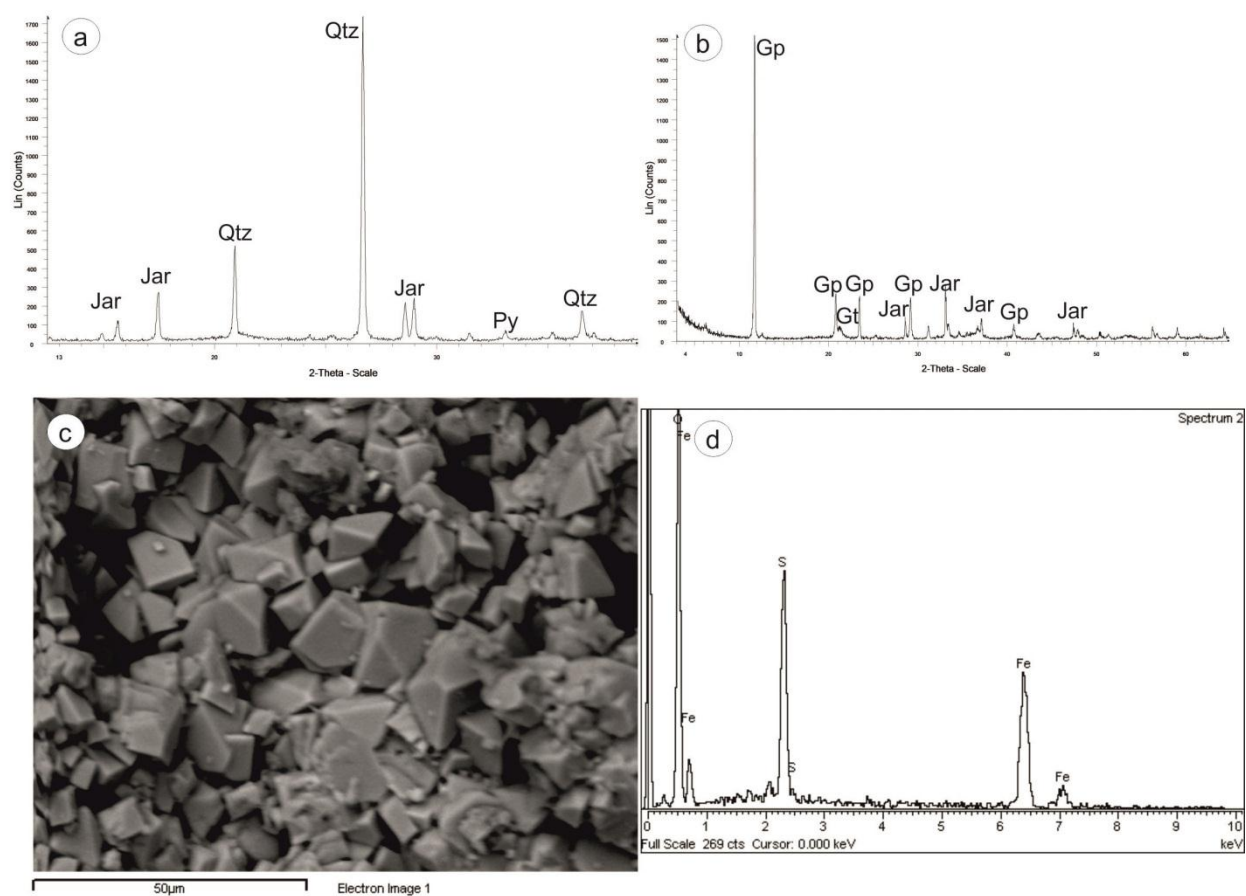


Fig. 3. (a) and (b) XRD patterns of mine waste samples (Jar: Jarosite; Qtz: Quartz; Py: Pyrite; Gp: Gypsum; Gt: Goethite); (c) BSE micrograph and (d) EDS spectrum of secondary Fe sulphate mineral in a mine waste sample.

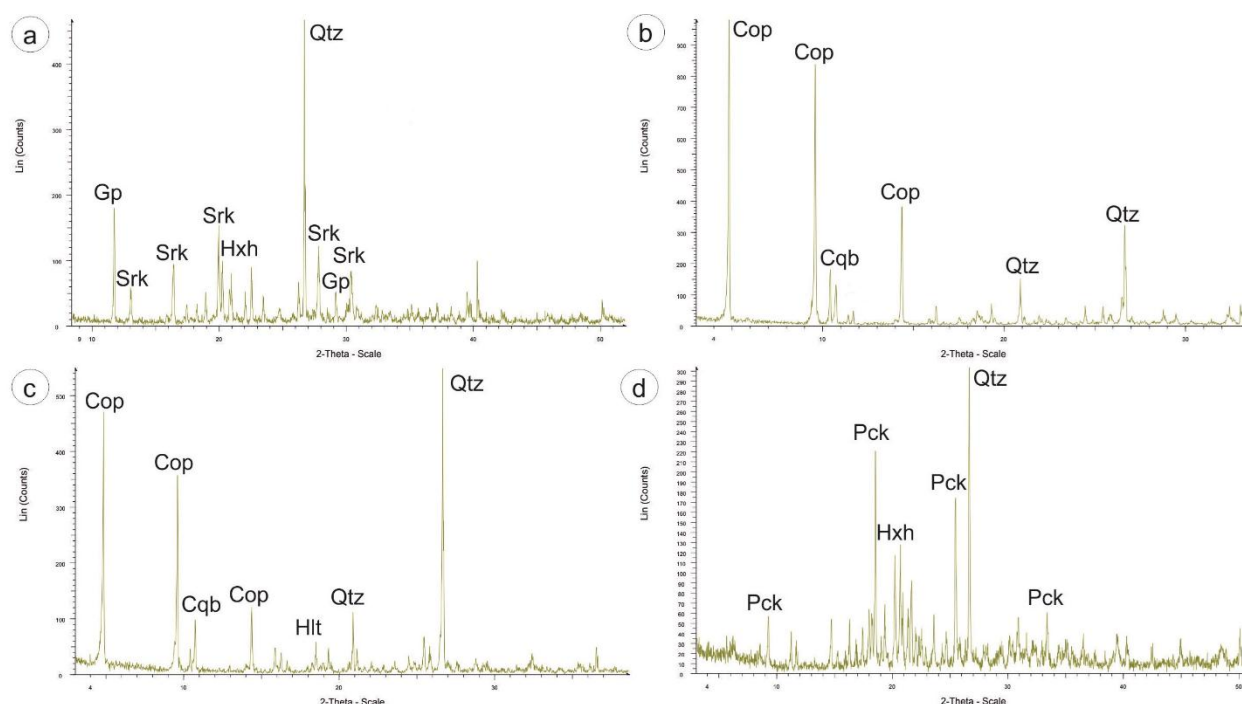


Fig. 4. XRD patterns of selected efflorescence samples from: **(a)** the Mathiatis lakeshore; **(b)** the Mathiatis Mine Waste Facility; **(c)** and **(d)** the Sha lakeshore (Qtz: Quartz; Gp: Gypsum; Srk: Starkeyite; Hxh: Hexahydrite; Cop: Copiapite; Cqb: Coquimbite; Hlt: Halotrichite; Pck: Pickeringite).

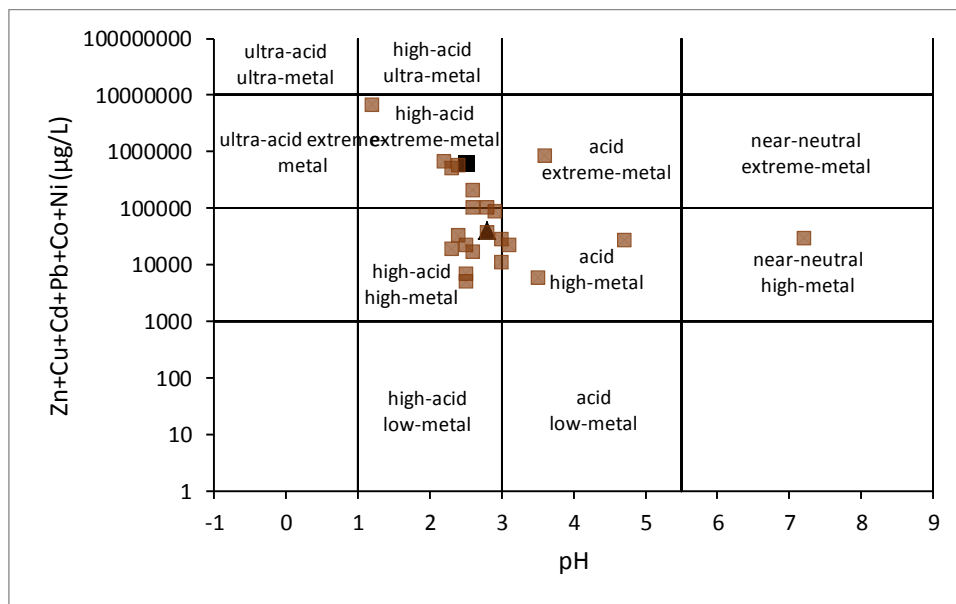
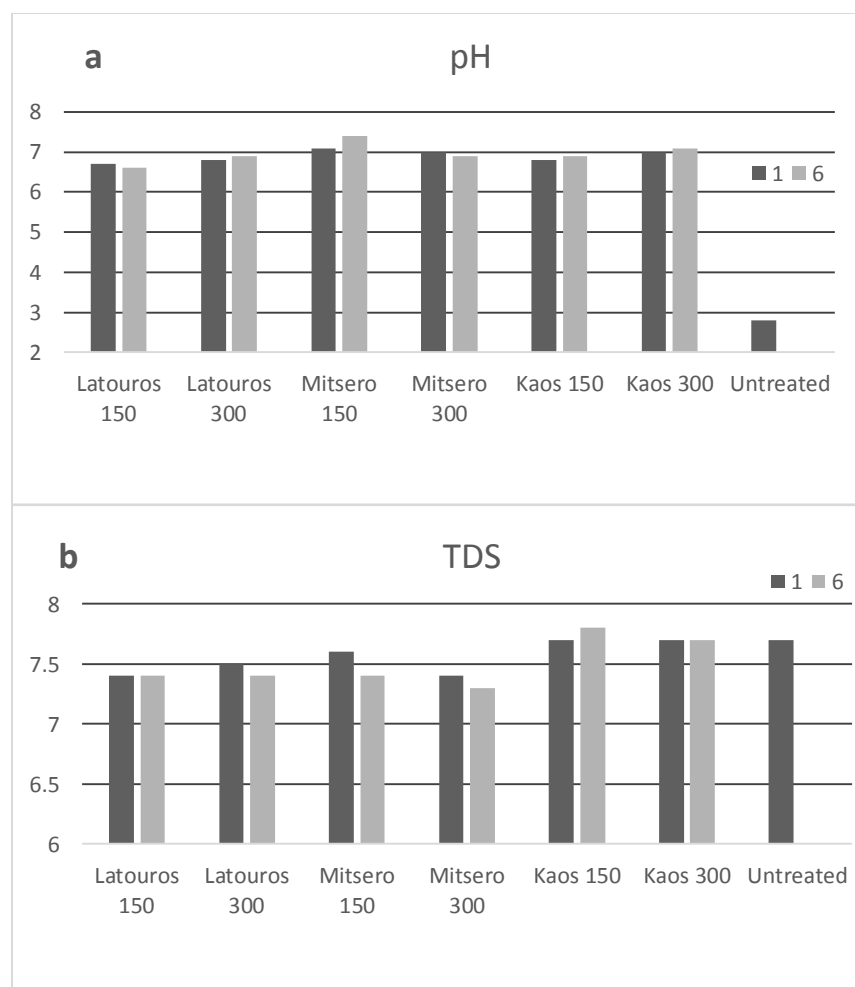


Fig. 5. Classification of the Mathiatis (black triangular) and Sha (black square) pit-lake water on the basis of the sum of dissolved base metal concentrations and pH. Additional data from IPB pit lakes (brown squares) from Sánchez-España *et al.* 2008. Classification scheme based on Ficklin *et al.* 1992; modified after Plumlee *et al.* 1999.



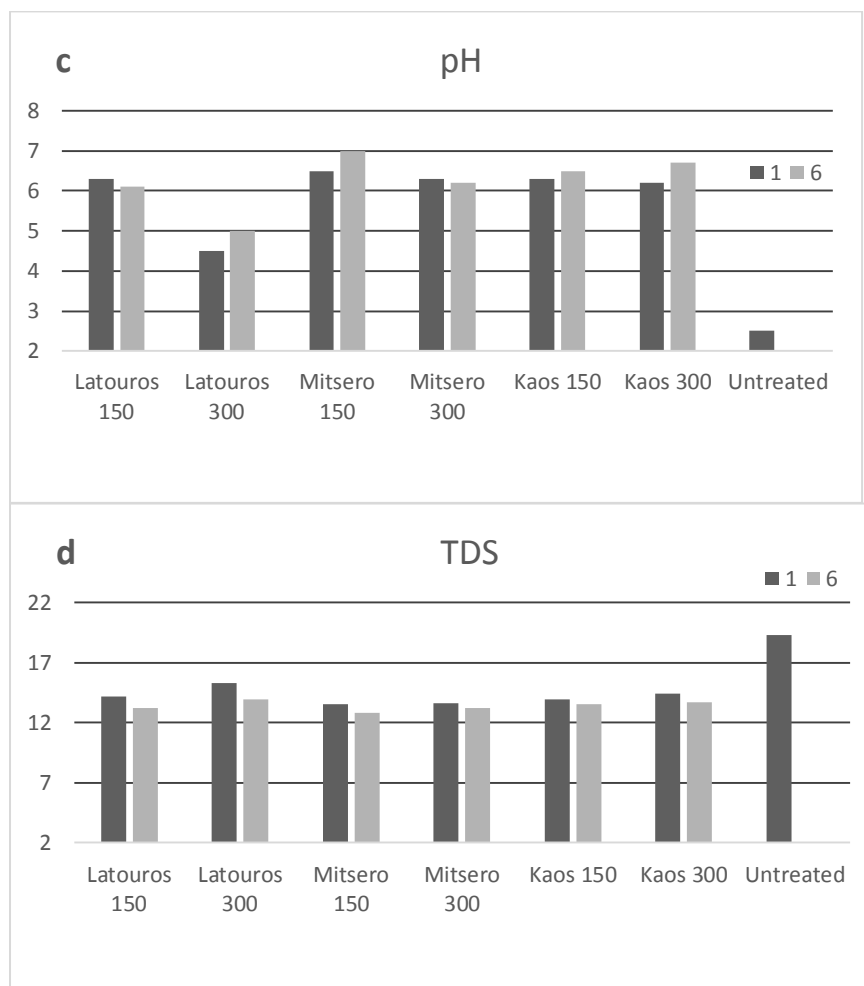
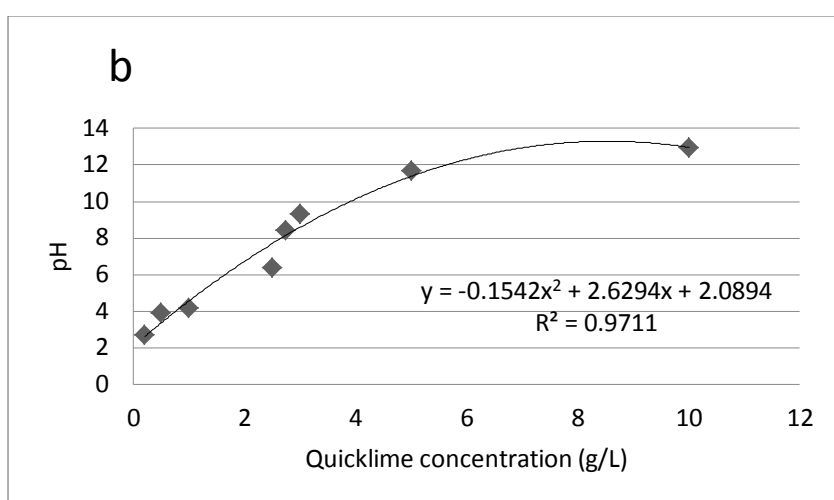
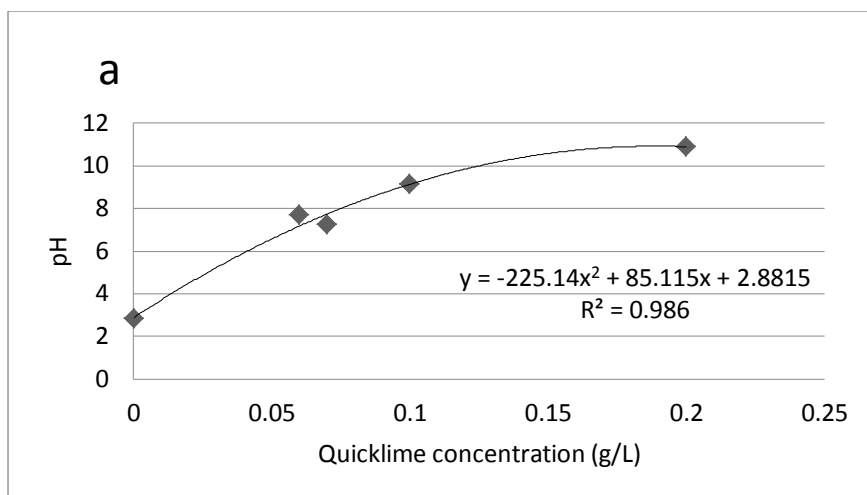


Fig. 6. Effect of limestone treatment on water pH and TDS after 1 and 6 hours reaction time.

Results for Mathiatis in (a), (b) and Sha in (c), (d).



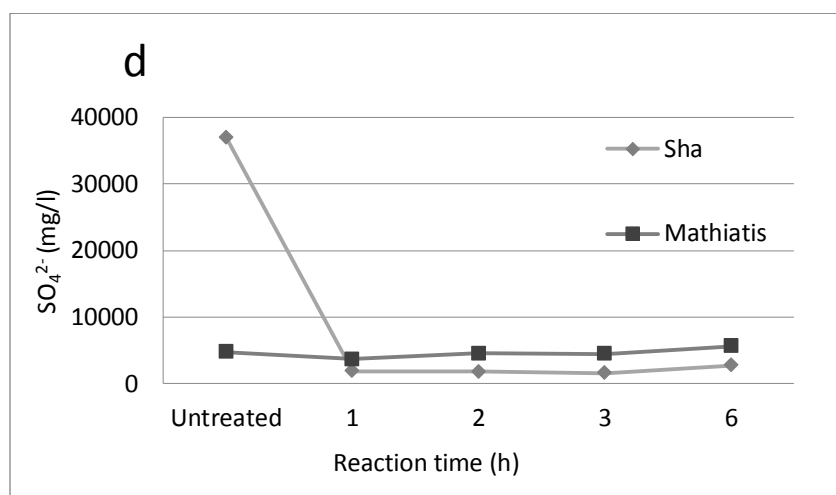
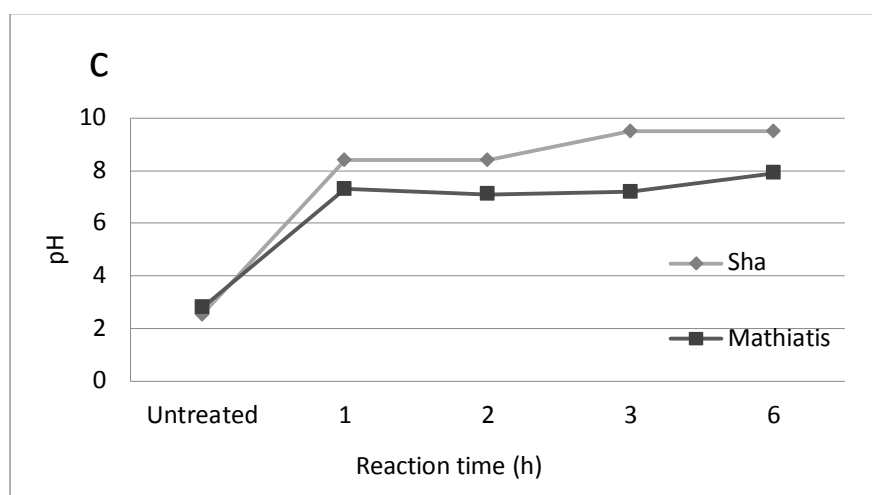


Fig. 7. Effect of quicklime concentration on pH of the Mathiatis (a) and Sha (b) pit-lake water and pH and SO_4^{2-} variation over time (c) and (d).

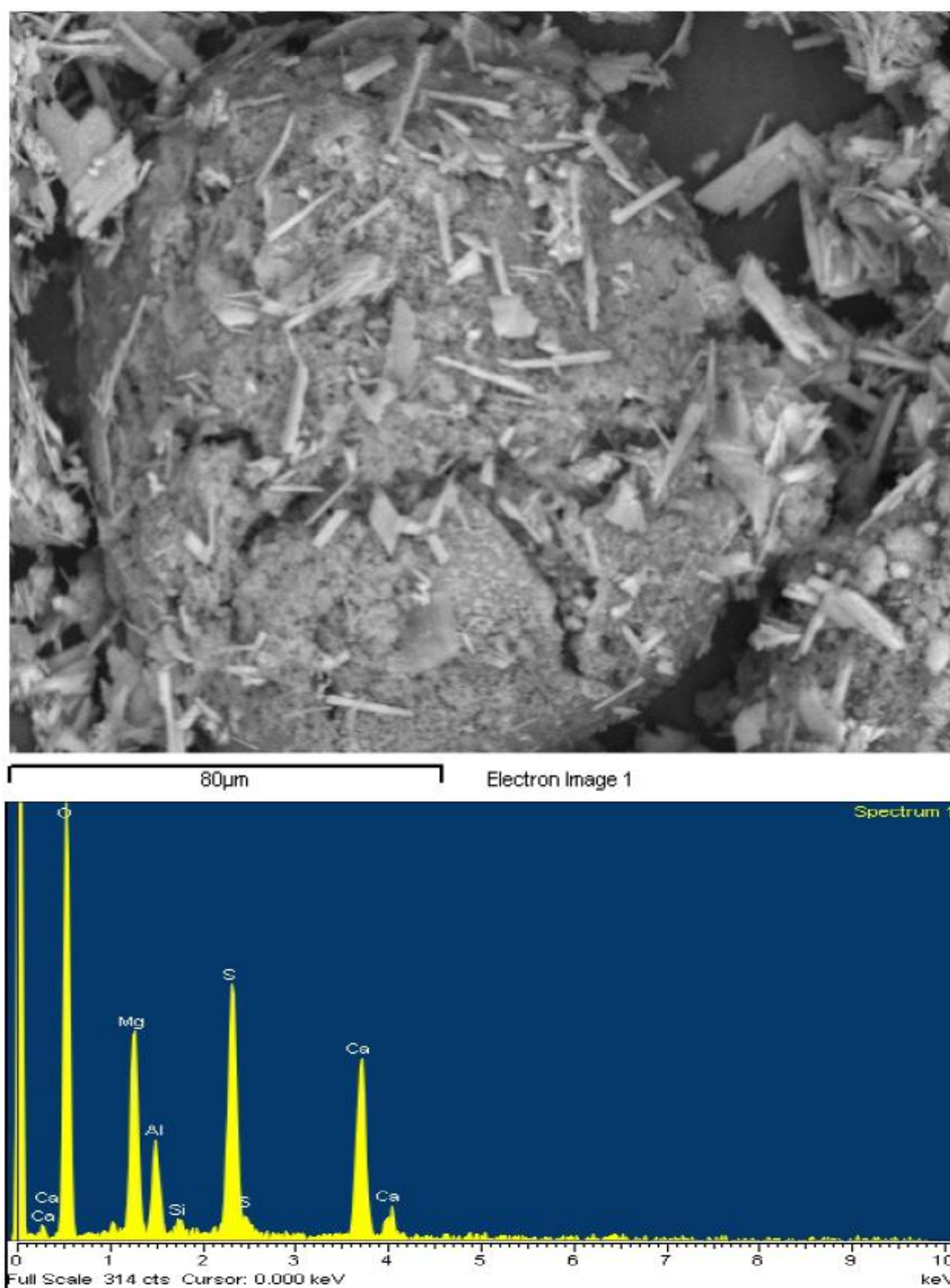


Fig. 8. The effect of armoring on a particle of quicklime. Platy crystals of gypsum are shown.

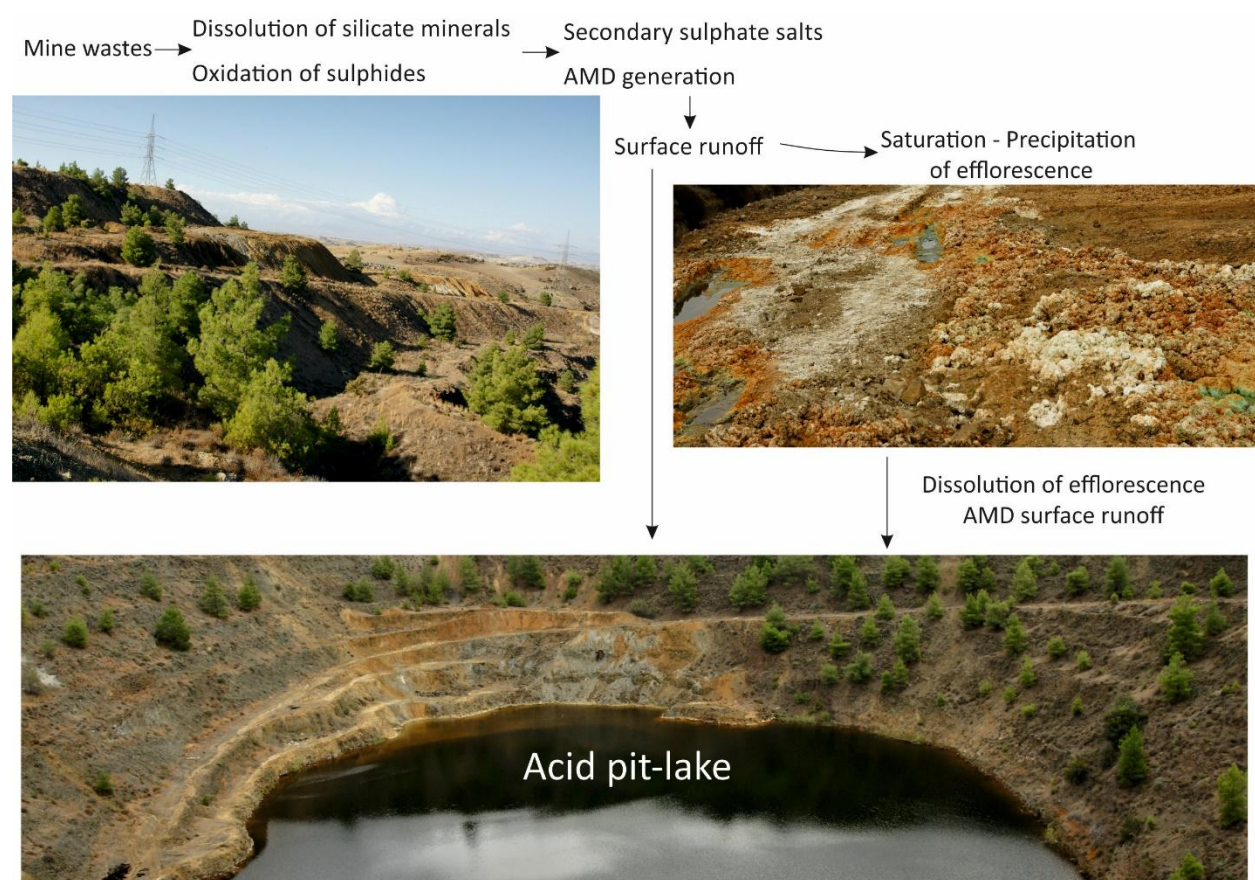


Fig. 9. Simplified visual representation of geochemical processes at the Mathiatis abandoned mine

Table 1. Chemical analysis of pyrite concentrates from the stockwork-type ore of Mathiatis and the massive sulphide ore of Sha. Analysis of the TAG Mount massive pyrite ore (Hannington et al. 1991) is given for comparison.

Sample No	Cu %	Fe %	S %	Zn %	Co %	As %	Au (mg/kg)	Ag (mg/kg)
Mathiatis								
MTO 1	0.05	37.0	42.1	0.06	0.01	0.02	0.76	<5
MTO 2	0.16	42.5	49.4	0.06	0.02	0.02	0.45	<5
MTO 3	0.09	31.1	35.4	0.01	0.10	<.005	0.16	<5
MTO 5	0.07	25.7	29.2	0.01	0.03	0.01	0.22	<5
Sha								
SHO 1	1.68	36.7	42.5	0.05	0.01	0.10	na	<5
SHO 3	4.27	16.3	18.9	0.01	0.01	0.09	na	7
SHO 4	0.07	21.8	24.9	0.01	0.01	0.02	1.1	15
TAG Mount	4.61	32.7	40.7	3.34	0.03	<0.01	1.43	37

na: not analysed; Pb <0.01 wt%; Mn<0.005 mg/kg; Ni<10 mg/kg; Cd<100 mg/kg; Hg<15 mg/kg; Sb<50 mg/kg

Table 2. *Summary table of the AP, NP and NNP values for the Mathiatis mine waste*

Sample	NaOH (ml)	NP (kg CaCO ₃ /t)	S (%)	AP	NNP
MTWM4	19.9	0.25	6.4	202	-202
MTWM4	19.8	0.50			-202
MTWM5	38.8	-46.95	10.4	329	-376
MTWM5	33.4	-33.47			-362
MTWM6	31.2	-27.95	4.8	151	-179
MTWM6	26.2	-15.50			-167
MTWM7	44	-59.78	7.6	242	-302
MTWM7	53.3	-83.12			-325

Table 3. *Chemical analyses and paste pH of the Mathiatis mine waste in comparison with the Dutch Intervention Limits (D.I.L.) (Swartjes 1999) and the average topsoil concentrations in Cyprus (Cohen et al. 2012)*

Sample	MTMW 4	MTMW 5	MTMW 6	MTMW 7	Average	D.I.L.	Cyprus topsoil average
Paste Ph	4.7	3.2	3.6	2.2	3.4	na	8.32
Al (%)	5.4	3.6	2.3	1	3.1	na	1.88
Ca (%)	1.8	2.6	1.3	0.6	1.6	na	11.9
Fe (%)	12	15.3	20.4	17.1	16.2	na	3.57
K (%)	0.5	0.3	0.2	0.1	0.3	na	0.24
Mg (%)	3.3	1.8	1.1	0.3	1.6	na	1.32
Na (%)	0.7	0.4	0.3	0.1	0.4	na	0.25
S (%)	6.4	10.4	4.8	9	7.7	na	na
Ag (mg/kg)	0.7	5.2	1.7	2.6	2.6	15	0.04
As (mg/kg)	31.5	82.9	159.6	83.8	89.5	76	4.9
B (mg/kg)	33.1	26.4	75.3	15.4	37.6	na	2
Ba (mg/kg)	5.6	6.4	12.8	7.4	8.1	8	163
Cd (mg/kg)	2.2	0.5	0.3	0.2	0.8	13	0.3
Co (mg/kg)	38.8	37.2	57.5	74	51.9	190	21.2
Cr (mg/kg)	23.5	14.1	16.9	4	14.6	na	73.7
Cu (mg/kg)	745	327	669	337	519	190	87.9
Hg (mg/kg)	0.2	0.8	0.3	0.4	0.4	36	0.03
Mn (mg/kg)	838	1529	12403	136	3727	na	981
Mo (mg/kg)	3.4	4.5	8.5	9.9	6.6	190	0.95
Ni (mg/kg)	26.5	26.3	69	4.9	31.7	100	111
Pb (mg/kg)	19.6	93.6	83.7	67.3	66	530	11
Sb (mg/kg)	1.7	5.2	4.2	4.3	3.8	22	0.41
Ti (mg/kg)	1117	676	761	334	722	na	900
V (mg/kg)	217	211	346	122	224	250	96
Zn (mg/kg)	1351	389	360	128	557	720	67

na: not available

Table 4. *Sulphate minerals in the Mathiatis and Sha abandoned mines*

Mineral	Nominal chemical formula*	Mathiatis Lakeshore	Mathiatis Mine Waste Facility	Sha Lakeshore
Mg sulphates				
Starkeyite	$\text{MgSO}_4 \cdot 4\text{H}_2\text{O}$	I	I	I
Pentahydrate	$\text{MgSO}_4 \cdot 5\text{H}_2\text{O}$	-	L	-
Hexahydrate	$\text{MgSO}_4 \cdot 6\text{H}_2\text{O}$	I	H	H
Mg-Al sulphate				
Pickeringite	$\text{MgAl}_2(\text{SO}_4)_4 \cdot 22\text{H}_2\text{O}$	L	H	I
Fe sulphates				
Copiapite	$\text{Fe}^{2+}\text{Fe}^{3+}_4(\text{SO}_4)_6(\text{OH})_2 \cdot 20\text{H}_2\text{O}$	L	H	L
Halotrichite	$\text{Fe}^{2+}\text{Al}_2(\text{SO}_4)_4 \cdot 22\text{H}_2\text{O}$	-	L	L
Coquimbite	$\text{Fe}^{3+}_2(\text{SO}_4)_3 \cdot 9\text{H}_2\text{O}$	-	I	L
Paracoquimbite	$\text{Fe}^{3+}_2(\text{SO}_4)_3 \cdot 9\text{H}_2\text{O}$	-	-	I
Szomolnokite	$\text{Fe}_2\text{SO}_4 \cdot \text{H}_2\text{O}$	-	L	-
Metasideronatrite	$\text{Na}_2\text{Fe}^{3+}(\text{SO}_4)_2\text{OH} \cdot 1-2\text{H}_2\text{O}$	-	L	-
Na-Mg sulphate				
Bloedite	$\text{Na}_2\text{Mg}(\text{SO}_4)_2 \cdot 4\text{H}_2\text{O}$	L	-	-
Na-Al sulphate				
Tamarugite	$\text{NaAl}(\text{SO}_4)_2 \cdot 6\text{H}_2\text{O}$	-	I	L
Al sulphate				
Alunogen	$\text{Al}_2(\text{SO}_4)_3 \cdot 17\text{H}_2\text{O}$	-	L	-
Ca sulphate				
Gypsum	$\text{CaSO}_4 \cdot 2\text{H}_2\text{O}$	H	H	L

Abundance: L low; I intermediate; H high

* Nominal chemical formula from Hammarstrom *et al.* 2005

Table 5. Physicochemical attributes and elemental concentrations of acidic pit-lakes and acid mine drainage

	Mathiatis pit-lake		Mathiatis LIFE Program pit-lake*		Sha pit-lake		Sha LIFE Program pit-lake*		Kalavasos AMD		Apliki pit-lake**		IPB pit-lakes§		Skorovas AMD¶	
	Mean	Range	Mean	Range	Mean	Range	Mean	Range	Mean	Range	Mean	Range	Mean	Range	Mean	Range
	n=6	n=2	n=4	n=2	n=1	n=5	n=62	n=1	n=1	n=5	n=62	n=1	n=62	n=1	n=1	n=1
pH	2.83	2.80-2.88	2.85-3.40	2.51	2.49-2.56	2.54-2.6	2.54-2.6	2.54-2.6	5.6	3.2	3.1-3.3	2.6	2.36	2.36	2.36	2.36
Eh (mV)	237	232-238	na	256	256-257	na	14.6-19.4	na	na	198	197-199	782	na	na	na	na
EC (mS/cm)	8	7.8-8.1	4.5-5.7	20.6	na	na	14.6-19.4	na	na	na	na	5.3	5.9	5.9	5.9	5.9
TDS (%)	7.6	7.5-7.6	na	19.3	na	na	na	na	na	na	na	na	na	na	na	na
SO ₄ (mg/L)	4764	4600-4850	2538-3055	37025	35900-38500	15890-31830	15890-31830	7410	16014	15480-16310	4000	7291	7291	7291	7291	7291
Cl ⁻ (mg/L)	690	637-810	445-600	106	57-133	200-225	200-225	na	na	na	na	na	na	na	na	na
Al (mg/L)	90	81-100	46	2626	2584-2653	1832	1832	7	na	169	164-174	91	na	na	na	na
As (µg/L)	<6	na	5	na	na	52-69	52-69	<6	na	na	na	na	na	na	na	na
B (mg/L)	5	4.0-5.0	1.0-3.0	<0.4	na	5.0-8.0	5.0-8.0	3.8	na	na	na	na	na	na	na	na
Ca (mg/L)	599	545-674	350-410	651	634-664	315-650	315-650	480	540	528-555	180	na	na	na	na	na
Cd (µg/L)	42	30-50	19-23	1220	1092-1337	810-1869	810-1869	10	633	600-700	102	519	519	519	519	519
Co (mg/L)	0.4	0.4-0.5	0.2-0.4	5.2	5.1-5.3	1.7-5.4	1.7-5.4	0.7	5.4	5.2-5.5	1.1	na	na	na	na	na
Cu (mg/L)	4	4.0-5.0	3.0-5.0	156	154-158	117-225	117-225	0.4	357	351-368	20	129	129	129	129	129
Fe (mg/L)	57	51-65	22-24	1025	1010-1042	229-538	229-538	1472	17	15-20	332	2284	2284	2284	2284	2284
K (mg/L)	2.5	2.0-3.0	3.6	<1	<1	0.4-4.5	0.4-4.5	7	12	43446	2	na	na	na	na	na
Mg (mg/L)	299	275-334	260-270	3455	3391-3500	1645-3375	1645-3375	775	2154	2100-2210	357	na	na	na	na	na
Mn (mg/L)	15	14-17	6.8	235	234-239	207	207	23	172	168-176	34	na	na	na	na	na
Na (mg/L)	1022	937-1131	600-915	161	158-162	160-265	160-265	1316	2048	1994-2122	31	na	na	na	na	na
Pb (µg/L)	65	40-140	3-58	480	420-520	2.0-14.0	2.0-14.0	<4000	na	na	122	na	na	na	na	na
Sr (mg/L)	1.2	1.1-1.4	0.7-0.8	0.5	0.52-0.54	0.4-0.6	0.4-0.6	2	na	na	na	na	na	na	na	na
Zn (mg/L)	35	32-39	20-23	448	441-453	313-567	313-567	77	66	64-68	31	256	256	256	256	256

* Charalambides et al. 1998; ** Antivachis et al. 2017; § Average chemical composition of 22 acidic mine pit-lakes from IPB (Sánchez-España et al. 2008); ¶ Banks et al. 1997

Table 6. *Elemental concentrations (mg/L) in treated pit-lake water after 6h of reaction time against various regulatory limits.*

Sample	Neutralization agent concentration (g/l)	Final pH	SO ₄ ²⁻	Cd	Co	Cr	Cu	Fe	Mn	Ni	Zn
Mathiatis pit-lake		2.83	4764	0.04	0.4	0.05	4.29	57.03	15.42	0.16	35.33
Kaos <150	100	6.9	5495	0.01	0.28	0.05	0.05	0.09	5.98	0.13	1.25
Latouros <300	100	6.9	4815	0.02	0.16	0.04	0.05	0.16	6.83	0.08	0.61
Mitsero <150	100	7.4	4650	0.01	0.18	0.05	0.04	0.11	4.28	0.06	0.53
Quicklime	0.7	7.9	3895	0.03	0.23	0.05	0.03	0.06	7.75	0.10	2.85
Sha pit-lake		2.51	37025	1.22	5.2	0.28	156.17	1025	235	3.62	448
Kaos <300	100	6.7	18250	0.27	2.55	0.27	0.22	0.59	159	1.13	19.3
Mitsero <150	100	7	19050	0.01	0.5	0.13	0.03	0.33	6.07	0.07	0.55
Quicklime	2.75	9.5	2750	0.01	0.03	0.03	0.03	0.07	0.01	0.03	0.02
Industrial and Agricultural use ⁽¹⁾⁽²⁾		6.5-9.5	250	0.005	0.05	0.05	0.2	3	0.2	0.02	2
Agricultural use ⁽³⁾				0.01	0.05	0.05	0.2	0.2	0.2	0.2	2
Drinking water ⁽⁴⁾		6.5-9.5		0.005	0.05	0.05	0.2	3	0.2	0.02	2
Drinking water ⁽⁵⁾		6.5-8.5		0.005	na	0.1	1.3	0.3	0.05	na	5

⁽¹⁾ Greek Ministerial Order (2009); ⁽²⁾ Greek Ministerial Order (2011); ⁽³⁾ Swartjes (1999); ⁽⁴⁾ Greek Common Ministerial Order (2001); ⁽⁵⁾ U.S.A. E.P.A. (2018)

Table 7. *Removal percentage of each element after 6h of reaction time*

Sample	Neutralization agent concentration (g/L)	Cd	Co	Cu	Fe	Mn	Ni	Zn
Mathiatis								
Kaos <150	100	76.00	31.25	98.95	99.82	57.64	16.13	96.03
Latouros <300	100	64.00	61.25	99.08	99.65	51.65	48.39	98.07
Mitsero <150	100	76.00	56.25	98.95	99.76	69.72	61.29	98.31
Quicklime	0.07	28.00	42.5	99.21	99.88	45.14	38.71	90.92
Sha								
Kaos <300	100	77.87	50.96	99.86	99.94	32.34	68.78	95.69
Mitsero <150	100	99.18	90.38	99.98	99.97	97.42	98.07	99.88
Quicklime	2.75	99.18	99.42	99.98	99.99	100.00	99.17	100.00